Cellular/Molecular

Perimenstrual-Like Hormonal Regulation of Extrasynaptic δ-Containing $GABA_A$ Receptors Mediating Tonic Inhibition and Neurosteroid Sensitivity

Chase Matthew Carver, Xin Wu, Omkaram Gangisetty, and Doodipala Samba Reddy
Department of Neuroscience and Experimental Therapeutics, College of Medicine, Texas A&M University Health Science Center, Bryan, Texas 77807

Neurosteroids are endogenous regulators of neuronal excitability and seizure susceptibility. Neurosteroids, such as allopregnanolone (AP; 3α-hydroxy-5α-pregnan-20-one), exhibit enhanced anticonvulsant activity in perimenstrual catamenial epilepsy, a neuroendocrine condition in which seizures are clustered around the menstrual period associated with neurosteroid withdrawal (NSW). However, the molecular mechanisms underlying such enhanced neurosteroid sensitivity remain unclear. Neurosteroids are allosteric modulators of both synaptic ($\alpha\beta\gamma_2$-containing) and extrasynaptic ($\alpha\beta\delta$-containing) $GABA_A$ receptors, but they display greater sensitivity toward δ-subunit receptors in dentate gyrus granule cells (DGGCs). Here we report a novel plasticity of extrasynaptic δ-containing $GABA_A$ receptors in the dentate gyrus in a mouse perimenstrual-like model of NSW. In molecular and immunofluorescence studies, a significant increase occurred in δ subunits, but not α_1, α_2, β_2, and γ_2 subunits, in the dentate gyrus of NSW mice. Electrophysiological studies confirmed enhanced sensitivity to AP potentiation of GABA-gated currents in DGGCs, but not in CA1 pyramidal cells, in NSW animals. AP produced a greater potentiation of tonic currents in DGGCs of NSW animals, and such enhanced AP sensitivity was not evident in δ-subunit knock-out mice subjected to a similar withdrawal paradigm. In behavioral studies, mice undergoing NSW exhibited enhanced seizure susceptibility to hippocampus kindling. AP has enhanced anticonvulsant effects in fully kindled wild-type mice, but not δ-subunit knock-out mice, undergoing NSW-induced seizures, confirming δ-linked neurosteroid sensitivity. These results indicate that perimenstrual NSW is associated with striking upregulation of extrasynaptic, δ-containing $GABA_A$ receptors that mediate tonic inhibition and neurosteroid sensitivity in the dentate gyrus. These findings may represent a molecular rationale for neurosteroid therapy of catamenial epilepsy.

Key words: **allopregnanolone; epilepsy; GABA receptor; neurosteroid; tonic inhibition; withdrawal**

Introduction

Neurosteroids play a key role in the pathophysiology of catamenial epilepsy, a menstrual cycle-related disorder characterized by seizures that cluster most often during the perimenstrual or periovulatory period, when progesterone levels are low (Herzog and Frye, 2003; Herzog et al., 2004, 2011; Reddy et al., 2012). Presently, there is no approved drug therapy for catamenial epilepsy. Progesterone is a precursor for the synthesis of neurosteroids, such as allopregnanolone (AP; 3α-hydroxy-5α-pregnan-20-one), in the brain (Reddy et al., 2004; Tuveri et al., 2008). AP and related neurosteroids have anticonvulsant properties and protect against seizures (Reddy, 2011). Although the exact cause of catamenial epilepsy is poorly understood, there is growing evidence suggesting that perimenstrual neurosteroid withdrawal (NSW) may be a key triggering factor for catamenial seizures (Smith et al., 1998a,b; Reddy et al., 2001, 2012; Reddy, 2009; Gangisetty and Reddy, 2010; Pack et al., 2011). Based on this approach, we have developed an animal model of catamenial epilepsy (Reddy et al., 2001, 2012; Reddy and Zeng, 2007). In this rodent model, there is a marked reduction in the antiseizure potency of benzodiazepines and valproate, which is consistent with clinical evidence on resistance of catamenial seizures to conventional antiepileptic drugs (Reddy and Rogawski, 2001; Gangisetty and Reddy, 2010; Reddy et al., 2012). However, we unexpectedly found that neurosteroids, including AP and synthetic analogs such as ganaxolone, had enhanced activity in the catamenial epilepsy model (Reddy and Rogawski, 2000, 2001; Reddy et al., 2012). We proposed a neurosteroid replacement therapy for prevention of catamenial seizures (Reddy and Rogawski, 2009; Reddy, 2013). However, the molecular mechanisms underlying enhanced anticonvulsant activity of neurosteroids in catamenial epilepsy remain unclear.

Neurosteroids control seizures through direct interaction with $GABA_A$ receptors ($GABA_A$Rs; Harrison and Simmonds, 1984; Belelli and Lambert, 2005; Hosie et al., 2007). $GABA_A$Rs are ligand-gated chloride channels that are composed of a pentamer of subunits (α1–α6, β1–β4, γ1–γ3, δ, ε, θ, and ρ1–ρ3). Synaptic, γ-containing receptors and extrasynaptic, δ-containing recep-

Received Feb. 12, 2014; revised Aug. 30, 2014; accepted Sept. 3, 2014.

Author contributions: C.M.C. and D.S.R. designed research; C.M.C., X.W., O.G., and D.S.R. performed research; C.M.C., X.W., and D.S.R. analyzed data; C.M.C., X.W., and D.S.R. wrote the paper.

This work was supported by National Institutes of Health Grant NS051398 (D.S.R.). We thank Dr. Martin Wallner for his kind donation of δ-subunit knock-out mice.

The authors declare no competing financial interests.

Correspondence should be addressed to Dr. D. Samba Reddy, Department of Neuroscience and Experimental Therapeutics, College of Medicine, Texas A&M University Health Science Center, 2008 Medical Research and Education Building, 8447 State Highway 47, Bryan, TX 77807-3260. E-mail: reddy@medicine.tamhsc.edu.

DOI:10.1523/JNEUROSCI.0596-14.2014

 0270-6474/14/3414181-17$15.00/0

tors have divergent roles in mediating phasic and tonic current inhibition, respectively (Bianchi and Macdonald, 2003; Wei et al., 2003; Semyanov et al., 2004). Neurosteroids produce large enhancing effects on δ-containing extrasynaptic receptors mediating tonic inhibition (Belelli et al., 2002; Wohlfarth et al., 2002; Stell et al., 2003; Pillai et al., 2004; Carver and Reddy, 2013). The δ-containing receptors in the hippocampus undergo plasticity during the menstrual cycle, pregnancy, and parturition (Maguire et al., 2005; Maguire and Mody, 2007, 2008; Zhang et al., 2007; Sanna et al., 2009; Wu et al., 2013). There are indications that steroid hormone fluctuations affect δ-subunit plasticity (Shen et al., 2005; Reddy et al., 2012). Therefore, we hypothesized that the enhanced potency of neurosteroids in catamenial epilepsy may be attributed to a relative increase in the expression of extrasynaptic, δ-containing $GABA_A$Rs in the hippocampus.

In this study, we tested this hypothesis by investigating NSW-induced changes in $GABA_A$R δ-subunit expression and tonic inhibition in the dentate gyrus (DG) in a mouse perimenstrual model. Our results demonstrate NSW-induced striking upregulation of δ-containing $GABA_A$Rs mediating tonic inhibition and conferring enhanced sensitivity to neurosteroids, similar to that observed in perimenstrual catamenial epilepsy.

Materials and Methods

Animals and perimenstrual model studies

Animals. Wild-type (WT) adult female C57BL/6 mice, with masses of 25–30 g each, were used in this study. Progesterone receptor knock-out (PRKO) mice were also used, and their generation has been described previously (Lydon et al., 1995; Reddy et al., 2004; Reddy and Mohan, 2011). PRKO mice lack both the PR-A and PR-B isoforms that are transcribed by the PR gene. $GABA_A$R δ-subunit knock-out mice (*Gabrd*$^{-/-}$; δKO) were a kind gift from Dr. Martin Wallner (University of California, Los Angeles, Los Angeles, CA) and were also used (Mihalek et al., 1999). All strains were maintained on a hybrid C57BL/6–129SV background. All mice were housed four to a cage with access to food and water *ad libitum*. The mice were housed in an environmentally controlled animal facility with a 12 h light/dark cycle. The animals were cared for in strict compliance with the guidelines outlined in the National Institutes of Health *Guide for the Care and Use of Laboratory Animals*. All animal procedures were performed in a protocol approved by the Institutional Animal Care and Use Committee of the university.

Perimenstrual model of NSW. A state of perimenstrual-like NSW hormonal condition was induced in animals by a standard progesterone–finasteride [*N*-(1,1-dimethylethyl)-3-oxo-(5α,17β)-4-azaandrost-1-ene-17-carboxamide] regimen as described previously (Reddy et al., 2010), which was based on published protocols for induction of NSW (Moran and Smith, 1998; Moran et al., 1998; Smith et al., 1998a,b). Adult female mice were given a subcutaneous injection of progesterone (25 mg/kg) twice daily for 7 d. On the final injection, finasteride (50 mg/kg, i.p.) was administered to block 5α-reductase activity for inhibiting progesterone conversion to AP and related neurosteroids. Progesterone was administered rather than AP because circulating levels of progesterone, such as those found during the luteal phase, are readily converted to neurosteroids in the brain regions that express neurosteroid synthesizing enzymes (Mellon et al., 2001; Agís-Balboa et al., 2006). The progesterone administration protocol results in a high physiological concentration of AP in plasma, and acute withdrawal is evident by a nearly complete decline in AP 24 h after finasteride administration (Gangisetty and Reddy, 2010). Control mice were administered 15% β-cyclodextrin vehicle with the same frequency for the 7 d injection period. Experimental studies were performed 24 h after the final finasteride or vehicle injection.

Molecular and cellular studies

TaqMan real-time PCR. The $GABA_A$R subunit mRNA expression was determined by the TaqMan real-time PCR assay as described previously (Gangisetty and Reddy, 2009). Mice were anesthetized with isoflurane, and the hippocampus was rapidly dissected for RNA isolation. The total RNA was extracted from the hippocampus using a TRIzol reagent, and cDNA was prepared using the Superscript II first-strand cDNA synthesis kit (Invitrogen). The PCR primers and TaqMan probe specific for $GABA_A$R subunits and GAPDH genes were designed using the Primer Express software (Applied Biosystems). TaqMan PCR reactions were performed in an AB 7500 fast real-time system (Applied Biosystems). Real-time PCR was performed with TaqMan Universal PCR Master Mix (Applied Biosystems), which contained AmpliTaq Gold DNA Polymerase, AmpErase, uracil N-glycosylase, dNTPs with dUTP, and optimized buffer components. Each sample was run in triplicate design, and each 25 μl reaction mixture consists of 12.5 μl of TaqMan Universal PCR Master mix, 400 nM primers, and 300 nM TaqMan probe for the target genes as described previously (Gangisetty and Reddy, 2009). The real-time PCR run consisted first of one cycle of 50°C for 2 min (AmpErase activation), then one cycle of 95°C for 10 min, 50 cycles of 95°C for 15 s, and 60°C for 1 min (denaturation, annealing, and extension). The target input amount for each target gene was normalized to GAPDH expression in the same samples to control for loading variability and then expressed as a percentage change with respect to mean control values in the same run. Brain tissue samples were collected from a group of 6–10 mice for each treatment condition.

Western blot analysis. Western blot analysis of $GABA_A$R subunit protein expression in the hippocampus was performed using affinity-purified rabbit polyclonal antibodies for $GABA_A$R α1, α2, α4, β2, and γ2 subunits (Santa Cruz Biotechnology) and δ subunit (PhosphoSolutions). Hippocampi were homogenized in RIPA buffer (Pierce), and the extracted protein (100 μg) was loaded onto 10% Tris-HCl gels and subjected to electrophoresis. Blots were then transferred to a polyvinylidene fluoride membrane (Bio-Rad). Membranes were blocked in 5% nonfat milk at room temperature for 1 h. Membranes were then incubated with $GABA_A$ subunit-specific antibody (dilution varies) or a mouse monoclonal β-actin antibody (1:1000) at 4°C overnight. Membranes were washed and incubated with an anti-rabbit antibody (1:1000) conjugated to horse radish peroxidase for 1 h at room temperature. Receptor subunit bands were detected using enhanced chemiluminescence reagent (PerkinElmer Life and Analytical Sciences). Protein bands were quantified using Alpha Imager software (Alpha Innotech). All values were normalized to β-actin expression in the same samples to control for loading amount variability and then expressed as a percentage change with respect to mean control values. Brain tissue samples were collected from a group of 6–10 mice for each treatment.

Immunocytochemistry and confocal microscopy. The δ-subunit distribution in the hippocampal neurons was determined by immunocytochemistry (Mangan et al., 2005; Wu et al., 2013). Acutely dissociated hippocampal CA1 pyramidal cells (CA1PCs) and dentate gyrus granule cells (DGGCs) from adult female mice in the vehicle and NSW groups were fixed with 4% paraformaldehyde for 15 min, followed by several glycine–PBS washes. Cells were permeabilized with ice-cold methanol for 3 min at 4°C followed again by several rinses with PBS. Cells were then incubated with blocking solution containing 1% bovine serum albumin (Vector Laboratories), 2.5% normal goat serum, and 0.1% Triton X-100 for 1 h. After the blocking, the cells were incubated together with primary rabbit $GABA_A$R δ subunits (1:100; PhosphoSolutions) or control rabbit IgG (1:100; Santa Cruz Biotechnologies) for 1 h at room temperature. Samples were rinsed and then incubated with Alexa Fluor 555-labeled secondary antibodies of goat anti-rabbit IgG (1:200; Invitrogen) for 1 h in the dark, washed extensively, and treated with ProLong AntiFade (Invitrogen). Serial image sections through focus with a step size of 0.1–0.3 μm thickness were collected and analyzed using a Nikon confocal microscope with NIS-Elements software suite (Nikon). The parameters for the confocal microscopy included the following: pinhole, 1 AU; the pixel dwell time, 0.5 frame/s; gain at the same level for sample and control IgG; power for the laser, 5%; and objective, Plan Apo VC 60× Oil DIC N2 (magnifying factor, −1.00; numerical aperture, 1.40; refractive index, 1.51). The normalized mean intensity was used as the ratio from mean intensity of $GABA_A$R δ subunits minus background to mean density of control antibody minus background. Mean intensity is a ratio of integrated density of the signal divided by the region of interest. Then nor-

malized mean intensity from the treatment group (NSW group) was used to compare with normalized mean intensity from the control group.

Electrophysiology studies

Hippocampal slice preparation. Transverse slices (300–400 μm thickness) of hippocampus were prepared using standard techniques from adult female mice. Mice were anesthetized with isoflurane, and brains were excised rapidly and placed in cold (4°C) artificial CSF (ACSF) buffer containing 0.3 mM kynurenic acid (Tocris Bioscience). ACSF buffer was composed of the following (in mM): 126 NaCl, 3 KCl, 2 $CaCl_2$, 2 $MgCl_2$, 26 $NaHCO_3$, 1.25 NaH_2PO_4, and 11 glucose (pH adjusted to 7.35–7.40 with 95% O_2–5% CO_2, 305–315 mOsm/kg). Hippocampal slices were cut with a vibratome in cold ACSF (model 1500 with 900 Refrigeration System; Leica Microsystems). The hippocampus was dissociated from the microdissected subfield tissues CA1, CA3, and DG, respectively. The tissue samples collected were rapidly frozen for RNA and protein extractions. For electrophysiology and immunocytochemistry studies, the microdissected subfield hippocampal slices were equilibrated in ACSF at 24°C and continuously bubbled with oxygen (95% O_2–5% CO_2). For each electrophysiology experiment, three to four animals were used for each group, and the drug concentration was tested.

Dissociation of neurons. Hippocampus CA1PC and DGGC dissociation was prepared by the standard dissociation technique described previously (Kay and Wong, 1986; Reddy and Jian, 2010; Wu et al., 2013). The hippocampal pieces of the CA1 or DG region were microdissected carefully under a microscope (model SMZ 647; Nikon) and incubated in ACSF for 1 h at 24°C. The isolated slices were transferred into an enzymatic solution consisting of ACSF with protease XXIII (3 mg/ml; Sigma-Aldrich). The slices were then incubated for precisely 23–25 min at 24°C. The remaining slices were rinsed twice with ACSF and gently triturated through three increasingly smaller, fire-polished Pasteur pipettes to yield single cells. For each batch, slices were triturated five or six times with each pipette in ~1 ml of ACSF. Then, the solution was allowed 1 min for the tissue to settle down, and the suspension of freshly dispersed cells were carefully plated onto the recording chamber (Warner Instruments) for electrophysiology and immunocytochemistry experiments.

Recording of GABA-evoked currents. Electrophysiological recordings were performed in the whole-cell patch-clamp configuration (Reddy and Jian, 2010; Wu et al., 2013). All electrophysiological experiments were performed at 22–24°C. The recording chamber was fixed into the stage of an inverted microscope with phase-contrast and differential interference contrast optics (model IX71; Olympus). The physiological bath solution for whole-cell recording had the following composition (in mM): 140 NaCl, 3 KCl, 10 HEPES, 2 $MgCl_2$, 2 $CaCl_2$, and 16 glucose, pH adjusted to 7.4 with NaOH (osmolarity, 315–325 mOsm/kg). Cells were visualized and images were acquired through a CCD-100 video camera (Dage-MTI) with FlashBus Spectrim 1.2 software (Pelco). Recording pipettes were pulled from capillary glass tubes (King Precision Glass) using a P-97 Flaming-Brown horizontal puller (Sutter Instruments). The pipette tip resistances were 2–4 MΩ for single-cell recording and 4–6 MΩ for slice recording. The recording pipettes were filled with a cesium pipette solution containing the following (in mM): 124 CsCl, 20 tetraethylammonium, 2 $MgCl_2$, 10 EGTA, 10 HEPES, 0.1 GTP, and 4 ATP, pH adjusted to 7.2 with CsOH (osmolarity, 295–305 mOsm/kg). In slice recordings, 5 mM lidocaine *N*-ethyl bromide (QX-314) was added to the pipette solution. Currents were recorded using an Axopatch 200B amplifier (Molecular Devices). The membrane capacitance, series resistance, and input resistance of the recordings were monitored by applying a 5 mV (100 ms) depolarizing voltage step from a holding potential of −70 mV for dissociated cells and −65 mV for slice recordings. Signals were low-pass filtered at 2 kHz and digitized at 10 kHz with the Digidata 1440A system. The current values were normalized to cell capacitance (an index of cell size) and expressed as current density (picoamperes per picofarads). For whole-cell current from isolated single cells, fractional potentiation produced by AP was calculated as I_A/I_{GABA}, where I_{GABA} was the response of peak amplitude at the application of GABA (3 μM), and I_A is the response of peak amplitude at the coapplication of GABA and the neurosteroid AP (0.01–1 μM). For fast application of test drugs, the perfusion pipette was positioned <200 μm away from the cell in the dish. GABA, AP, and the $GABA_A$R competitive antagonist bicuculline (10 μM) were applied using a multichannel perfusion system (Automate Scientific).

Tonic current recording and analysis. The $GABA_A$R-mediated tonic current recording and analysis were made as described previously (Mtchedlishvili and Kapur, 2006; Wu et al., 2013). Hippocampal slices (300 μm) were maintained in continuously oxygenated ASCF at 32°C in a holding chamber for 60 min, and then recordings were made at room temperature. Hippocampal CA1PCs and DGGCs were visually identified with an Olympus BX51 microscope equipped with a 40× water-immersion objective, infrared differential interference contrast optics, and a video camera (Kay and Wong, 1986). Tonic current and phasic miniature IPSCs (mIPSCs) of $GABA_A$Rs were recorded in the presence of tetrodotoxin (TTX; 0.5 μM, Na^+ channel blocker and inhibition of action potential-evoked neurotransmitter release), D,L-2-amino-5-phosphonovaleric acid (APV; 40 μM, NMDA channel blocker; Sigma), and 6,7-dinitroquinoxaline-2,3-dione (DNQX; 10 μM, non-NMDA glutamate receptor blocker). The competitive antagonist gabazine (GZ; SR-95531 [2-(3-carboxypropyl)-3-amino-6-(4-methoxyphenyl) pyridazinium bromide]; 50 μM) was added to perfusion after slice recordings to confirm block of GABAergic currents.

Offline current analysis was performed with pClamp 10.2 software (Molecular Devices) and in-house software. To study the tonic inhibition, transient events were manually removed from the current trace, so that it consisted only of membrane current in the voltage-clamp mode (Mtchedlishvili and Kapur, 2006; Wu et al., 2013). The averaged amplitude of tonic current shift in conductance and root mean square (RMS) noise amplitude were measured. The $GABA_A$R tonic current was expressed as the outward shift in holding current after application of GZ (50 μM). Currents for a single cell were normalized to membrane capacitance for that cell (picoamperes per picofarads). The amplitude of RMS (I_{RMS}) is the noise conductance from chloride ions passing through the opened channels and in proportion to the chloride driving force. I_{tonic} was measured and averaged in 100 ms epochs with 1 s intervals between epochs for 30 epochs. The measurements were taken 30 s before and 2–3 min after application of a drug. I_{RMS} was studied in 50 ms epochs with 500 ms intervals between epochs for 30 epochs before and after drug application in each cell. To assess the effect of a drug on I_{RMS} in an individual neuron, the distribution of I_{RMS} in 30 epochs before the application of a drug (during the baseline period) was compared with that after drug application by a Student's independent *t* test. To compare data obtained from a group of neurons, I_{RMS} values in individual epochs before and after drug application were averaged. Changes in I_{tonic} or I_{RMS} are expressed in picoamperes of current.

For measurement of desensitization of extrasynaptic current, traces were fit using a standard exponential function ($f(t) = A \times e^{-t/\tau} + C$) with the Chebyshev fitting method in Clampfit 10.2 software (Molecular Devices) with $r^2 \geq 0.95$. The asymptote of desensitization was described with regression analysis. The time point reaching within 10% of the arbitrary finite limit was designated the beginning time point measurement for the desensitized tonic current, averaged in 100 ms epochs with 1 s intervals between epochs. Percentage change of tonic current at the peak and desensitized points was then compared.

Miniature postsynaptic current data analysis. mIPSCs were detected using offline analysis with Mini-Analysis software (Synaptosoft), with the threshold for detection set at least three times the baseline RMS noise. mIPSC characteristics of amplitude, frequency, and decay time constants were determined and compared between groups as described previously (DuBois et al., 2013), adapted for granule cells. mIPSCs were acquired for 3 min for each drug response and condition. The decay of averaged mIPSCs within DG granule cells was best fit with a double-exponent time constant (Stell et al., 2003). Non-overlapping events with single peaks were used to generate an ensemble average mIPSC by aligning the rising phase and the 10–90% decay phase for each neuron and fit with the biexponential function: $I(t) = A_1 \times e^{(-t/\tau 1)} + A_2 \times e^{(-t/\tau 2)}$, where A_1 and A_2 are the fast and slow component amplitudes, and τ_1 and τ_2 are their respective time constants. A mean weighted decay constant was determined as $\tau_w = (A_1 \times \tau_1 + A_2 \times \tau_2)/(A_1 + A_2)$, as specified previously (Sun et al., 2007). The mean values in response to drug application were established for each recorded neuron, and the results are expressed

as mean ± SEM for each group, with comparisons between groups made using Student's *t* test. Comparisons of cumulative probability distributions were made using the Kolmogorov–Smirnov test. Results were considered significant if the two-tailed *p* values were <0.05.

Behavioral studies

Hippocampus kindling seizures. The kindling model of epileptogenesis was used for assessment of seizure susceptibility during the NSW period. The rapid kindling model allows accelerated evaluation of experimental manipulations during the progression of seizure induction (Reddy and Mohan, 2011; Wu et al., 2013). Electrode implantation and stimulation procedures for mouse hippocampus kindling were performed as described previously (Reddy and Mohan, 2011). Mice were anesthetized by an intraperitoneal injection of ketamine (100 mg/kg, i.p.) and xylazine (10 mg/kg, i.p.). A stimulation-recording bipolar electrode (model MS303/1; Plastics One) was stereotaxically implanted in the right ventral hippocampus (2.9 mm posterior, 3.0 mm lateral, and 3.0 mm below dura) using the atlas of Franklin and Paxinos (1997). The electrode was anchored with dental acrylic to three small screws placed in the skull. After a postoperative recovery period of at least 1 week, the electrographic afterdischarge (AD) threshold was determined by an application of 1 ms duration of biphasic rectangular pulses at 60 Hz for 1 s, beginning at 25 μA by using an isolated pulse stimulator (A-M Systems). AD duration was the total duration of hippocampus electrographic spike activity (amplitude $>$ 2× baseline) occurring in a rhythmic pattern at a frequency $>$1 Hz. Additional stimulations increasing in increments of 25 μA were given at 5 min intervals until an electrographic AD duration lasting at least 5 s was detected using the digital EEG system (Astro-Med). Mice were stimulated at 125% AD threshold (1-ms-duration pulse, 60 Hz frequency for 1 s) at 30 min intervals until they showed stage 5 seizures, which is considered the fully kindled state (Reddy and Mohan, 2011). Stimulations were delivered every 30 min until stage 5 seizures were elicited on three consecutive trials. For AP treatment studies, mice were stimulated once per day until stage 5 seizures were elicited on 3 consecutive days. The electrographic activity and AD duration were acquired from the hippocampal electrode using Axoscope 8.0 software with Digidata 1322A interface (Molecular Devices) through a Grass CP511 preamplifier (Astro-Med). Behavioral seizures were rated according to Racine's scale (Racine, 1972) as modified for the mouse: stage 0, no response or behavior arrest; stage 1, chewing or facial twitches; stage 2, chewing and head nodding; stage 3, forelimb clonus; stage 4, bilateral forelimb clonus and rearing; stage 5, falling. During each stimulation session, the behavioral seizure score and the AD duration were noted. Rate of kindling development, that is, numbers of stimulation required to induce stage 5 seizures, was determined in rapidly kindled mice subjected to NSW. Cumulative AD duration was calculated as an index of total seizure activity for reaching stage 5 seizures. Kindling experiments were conducted in a group of mice consisting of 6–15 mice for each treatment or genotype.

Antisense oligonucleotide administration. $GABA_A$R δ-subunit antisense treatments were given via intracerebroventricular microinfusion in the lateral ventricle in WT mice. Phosphorothioated antisense (5′-CGT-TTG-TAC-CTT-ATG-TGG-TA-3′) oligonucleotides were used to block δ-subunit-containing $GABA_A$R expression as described previously (Maguire et al., 2005). The missense oligonucleotide to δ-subunit mRNA (5′-AT-GGT-GTA-TTC-CAT-GTT-TGC-3′) was used as a control. Along with a bipolar electrode in the hippocampus, a 26-gauge guide cannula (Plastics One) was stereotaxically implanted into the lateral ventricle (0.5 mm posterior, 1.5 mm lateral, and 2.0 mm below dura) of mice for oligonucleotide administration. After a period of at least 1 week of recovery, dual-implanted animals were subjected to kindling stimulation. HPLC purified antisense oligonucleotides (IDT) were dissolved in sterile saline and injected in a 5 μl volume into the lateral ventricle using a perfusion pump. Fully kindled mice were infused with either 5 nmol of δ missense mRNA or 5 nmol of δ antisense mRNA at the time of finasteride administration, and behavioral studies were performed 24 h after NSW. These experiments were conducted in a group of mice consisting of six to nine mice for each treatment.

Drugs and reagents. All chemicals used in the electrophysiology studies were purchased from Sigma-Aldrich unless otherwise specified. Stock solutions were diluted in the external perfusion solution to the desired concentration for electrophysiological use. Stock concentrations of GABA, SR-95531, bicuculline methiodide, APV, DNQX, TTX, and 4,5,6,7-tetrahydroisoxazolo[5,4-c]pyridin-3-ol hydrochloride (THIP; gaboxadol) were dissolved in water, and AP was prepared in dimethylsulfoxide. The concentration of dimethylsulfoxide in the final solution was $<$1%. AP, progesterone, and finasteride were acquired from Steraloids. Kynurenic acid and THIP were acquired from Tocris Bioscience. TTX was procured from Calbiochem. Progesterone (25 mg/kg) and finasteride (50 mg/kg) solutions were made in 15% β-cyclodextrin w/v in water. Drugs were administered to animals subcutaneously or intraperitoneally in a volume equaling 1% of the animal's body weight.

Statistical analysis. Group data were expressed as the mean ± SEM. The $GABA_A$R subunit expression was analyzed based on a relative quantification approach as described previously (Gangisetty and Reddy, 2009). Statistical comparisons of electrophysiology and expression group data were performed using an independent two-tailed Student's *t* test, followed by Tukey's HSD test *post hoc*. In all statistical tests, the criterion for statistical significance was $p < 0.05$, unless otherwise specified. For acutely dissociated neuron current recordings, fractional potentiation produced by AP was calculated as I_A/I_{GABA}, where I_{GABA} is the peak current amplitude of the control GABA response, and I_A is the peak current response of the coapplication of GABA and the allosteric drug. A control GABA concentration of 3 μM evoked 10% of the maximal inhibitory current (EC_{10}), as determined previously in native, murine CA1PCs (Reddy and Jian, 2010). The concentration of allosteric modulator producing half of the maximal increase in the amplitude of the GABA response (EC_{50}) was determined by fitting the concentration–response relationships to the following nonlinear sigmoid Hill function: $I/I_{max} = [1 + (EC_{50}/[A])^n]^{-1}$, where *A* is the allosteric modulator concentration, I_{max} is the current evoked by GABA in the presence of a maximal potentiating concentration of the allosteric modulator, *I* is the current produced by GABA in the presence of a concentration *A*, EC_{50} is the concentration of *A* required to produce half of its own maximal GABA potentiating effect, and *n* is the Hill coefficient. Concentration–response curve data were subjected to nonlinear, logistic fitting. A Hill curve fitting was acquired only for concentration responses that achieved a plateau in maximum current response.

Results

NSW induces upregulation of $GABA_A$R δ-subunit expression

To simulate the perimenstrual-like hormonal milieu in mice, we first created a condition of prolonged, elevated progesterone and neurosteroids to model the luteal phase and then induced an abrupt decline in neurosteroid levels to more closely model perimenstrual changes in women (Fig. 1). This paradigm is consistent with perimenstrual catamenial epilepsy in which patients experience NSW (Reddy et al., 2012; Reddy, 2013).

To determine the withdrawal-induced changes in δ-subunit plasticity in the hippocampus, we performed TaqMan real-time PCR assay and Western blot analysis of receptor subunit expression in the hippocampus. Expression of δ subunit and its partnering α4 subunit was significantly increased in the DG after withdrawal compared with vehicle-injected control animals (Fig. 2*A*). We further quantified this NSW-induced expression by delineating upregulation specific to the hippocampus subfields CA1, CA3, and DG (Fig. 2*B*,*C*,*D*). There were no significant changes in hippocampal expression of other receptor subunits, including α_1, α_2, β_2, and γ_2 (Fig. 2*A*). The mean mRNA copy number of δ subunit within the DG was more than threefold greater than in CA1 and CA3 subfields (Fig. 2*B*). Protein levels of δ subunit in the DG were increased in NSW animals relative to controls as detected by Western blot analysis with a δ-specific antibody (relative protein expression, 1.00 ± 0.11 control vs

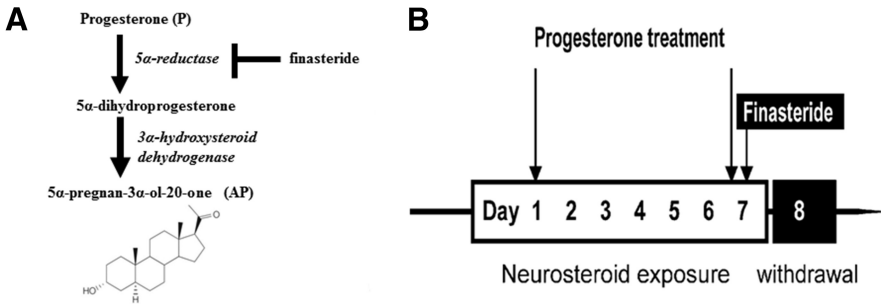

Figure 1. Overview of AP synthesis and perimenstrual-like NSW paradigm. ***A***, Abrupt inhibition of AP synthesis was accomplished by pharmacological blockade of 5α-reductase activity with finasteride. ***B***, In the perimenstrual model, progesterone was administered twice daily for 7 d, and finasteride was administered on the final day, resulting in NSW. Molecular and electrophysiology studies were done 24 h after induction of withdrawal.

4.56 ± 0.22 NSW, $p = 0.0001$; Fig. 2*E*,*F*). The α_2 and γ_2 mRNA expression in the DG was not significantly different between NSW and control. Subunit γ_2 mRNA expression percentage was 79.8 ± 17.0% in NSW tissue compared with 100.0 ± 12.6% in control DG tissue ($p = 0.3562$), and subunit α_2 mRNA percentage expression was 82.4 ± 10.5% in NSW tissue compared with 97.0 ± 8.4% in control tissue ($p = 0.2958$). Overall, these findings indicate a marked increase in the expression of δ subunit in the DG after NSW in the mouse perimenstrual-like paradigm.

To confirm the elevation of δ-containing receptors within the hippocampus, we visualized and determined the single-cell distribution of δ subunit by fluorescent immunocytochemistry using a δ-specific primary antibody. Staining with the antibody showed broad distribution of δ subunit on the soma, axon, and dendritic regions of acutely dissociated CA1PCs and DGGCs acquired from NSW and control mice (Fig. 3*A*). The normalized mean intensity, expressed as percentage change in fluorescence mean intensity of δ-subunit staining relative to the mean intensity of control IgG (for details, see Materials and Methods), was significantly greater in DGGCs of NSW mice compared with control animals (Fig. 3*B*, $p < 0.05$). The percentage change of immunofluorescence between control and NSW DGGC (77.1 ± 1.3%) was significantly greater than the change in CA1 cells attributed to NSW (13.4 ± 2.1%; $p < 0.05$). The δ-subunit protein was concentrated on cell membrane from the *x*–*z* and *y*–*z* axes obtained from confocal microscopy, as demonstrated previously (Wu et al., 2013).

The lack of significant increase to δ-subunit expression in CA1 is contradictory to previous findings of increased δ and α4 in the CA1 of steroid-withdrawn pubertal mice (Shen et al., 2007). However, our findings represent plasticity in adult females, and the discrepancies could be related to age differences between the mouse models used or other experimental factors. From mouse neonates to adulthood, granule cells undergo increased GABA and AP affinity and potency, denoting substantial $GABA_AR$ expressional changes across development (Mtchedlishvili et al., 2003). The discrepancies could be related to the mode of sample collection or sensitivity of assay method used for estimating subunit plasticity. We used a highly sensitive TaqMan PCR for analysis of receptor subunit expression in microdissected tissue sample. Our data are consistent with the expression pattern of δ subunit, which is expressed in relative abundance in the DG compared with other hippocampus subfields (Brickley and Mody, 2012).

NSW increase in δ subunit occurs via a PR-independent pathway

To determine whether the PRs are involved in regulating δ-subunit expression in response to NSW, we used homozygous PRKO mice that lack PR-A and PR-B receptor subtypes in the brain (Reddy et al., 2004). In PRKO mice, NSW resulted in a significant increase of δ-subunit expression (334 ± 39% NSW vs 83 ± 7% control; $p < 0.01$), similar to that observed with WT NSW mice (224 ± 37% NSW vs 100 ± 12% control; $p < 0.01$). These data were collected from 8–10 animals per strain and condition. These results indicate that NSW upregulation of δ subunit in the DG occurs in a PR-independent pathway.

NSW confers enhanced sensitivity to the neurosteroid AP potentiation of whole-cell GABA-gated currents in DGGCs

To confirm a functional role for NSW-induced expression of δ-containing $GABA_ARs$, we recorded whole-cell, GABA-gated currents in acutely dissociated DGGCs and CA1 pyramidal neurons with voltage-clamp patch electrophysiology (Fig. 4). There are previous reports of δ-subunit-containing receptors with submicromolar GABA affinities (Mortensen et al., 2010; Meera et al., 2011); however, these aforementioned studies were conducted in heterologous expression systems using recombinant $GABA_ARs$. The effective concentration value depicted in the dissociated experiments in Figure 4 was derived from concentration–response curves for native, murine hippocampal neurons (Reddy and Jian, 2010; Wu et al., 2013). This range of GABA affinity is consistent with previous reports within adult mouse granule cells in which the GABA EC_{50} is 18–20 μM and the EC_{10} value is >1 μM (Mtchedlishvili et al., 2003). GABA at 3 μM is at the upper limit of the detected range of extracellular GABA *in vivo* (Lerma et al., 1986), and δ-containing receptors shift from low-efficacy to high-efficacy gating during neurosteroid interaction (Bianchi and Macdonald, 2003). Thus, 3 μM GABA (EC_{10}) was applied to establish a control agonist current for each cell without producing significant receptor desensitization (Reddy and Jian, 2010). Increasing concentrations of AP (0.01–1 μM) were then coapplied with 3 μM GABA. A 2 min washing interval was implemented between each neurosteroid application for adequate drug removal and minimization of receptor desensitization.

AP elicited a concentration-dependent potentiation of GABA current in both the CA1 and DGGC (Fig. 4*A*). These currents were blocked by bicuculline (data not shown), indicating that they are mediated by $GABA_ARs$. Rapid application of AP in the absence of GABA did not produce gating of current. Allosteric potentiation of receptors by AP was measured as fractional potentiation I_A/I_{GABA}, where I_{GABA} was the peak current amplitude response to 3 μM GABA alone, and I_A was the peak current amplitude of GABA coapplied with AP (Wu et al., 2013). Data were compiled from 8 to 16 cells for each AP concentration and neuron type. CA1PCs from control and NSW animals displayed similar levels of AP-mediated fractional potentiation with no significant differences between conditions at any of the tested concentrations (Fig. 4*B*). In NSW DGGC, AP (0.1–1.0 μM) produced a greater potentiation of GABAergic current than in the vehicle control DGGCs (Fig. 4*C*). There was no current–response plateau despite increasing concentrations of AP. AP concentrations >1 μM were not tested because of the ability of neurosteroids to directly activate $GABA_ARs$ at higher concentrations via a separate binding domain (Majewska et al., 1986; Wohlfarth et al., 2002; Reddy and Rogawski, 2002).

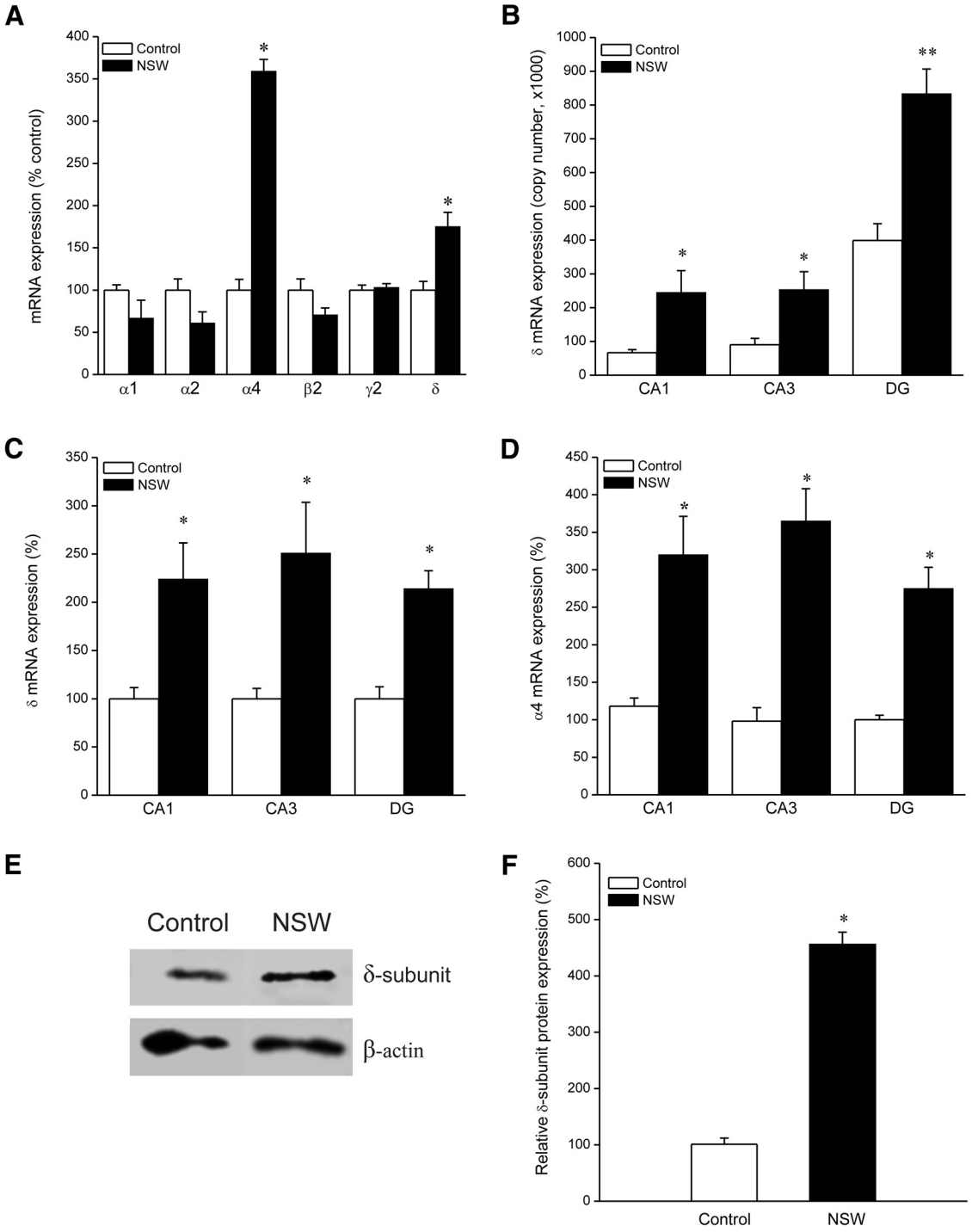

Figure 2. Upregulation of $GABA_AR$ δ-subunit expression in the hippocampus in mice undergoing perimenstrual NSW. ***A***, Whole-hippocampus δ mRNA expression increased in NSW female mice compared with vehicle-injected control animals as measured by TaqMan real-time PCR. ***B***, NSW significantly increased δ mRNA copy number in all three hippocampal subregions of the CA1, CA3, and DG. The δ copy number was more abundant and proliferative in the DG than the CA1 or CA3. ***C***, NSW significantly increased δ mRNA percentage expression in the CA1, CA3, and DG. ***D***, NSW significantly increased α4 mRNA expression in hippocampus subfields. ***E***, ***F***, NSW increased δ-subunit protein levels in the DG as denoted by representative Western blot analysis and relative quantification. $^*p < 0.05$ versus control; $^{**}p < 0.01$ versus control ($n = 6$–10 mice per group).

NSW confers enhanced extrasynaptic $GABA_AR$-mediated tonic currents in DGGCs

The DG upregulation of δ subunit in NSW is most functionally significant at extrasynaptic sites, in which these receptor subunits preferentially localize and coassemble with α4 on the membrane surface (Sun et al., 2004), with a denser staining in the molecular layer than the granule layer (Peng et al., 2002). To further confirm the functional significance of elevated levels of δ-subunit expression on extrasynaptic GABAergic network inhibition, we recorded GABA-gated tonic currents from WT DGGCs in a hippocampal slice preparation, in which synapses and dendritic connections remain functional. Bath perfusion of ACSF contained 0.5 μM TTX to block action potentials. We examined tonic current modulation of GABA, THIP, and 1 μM GABA coapplied

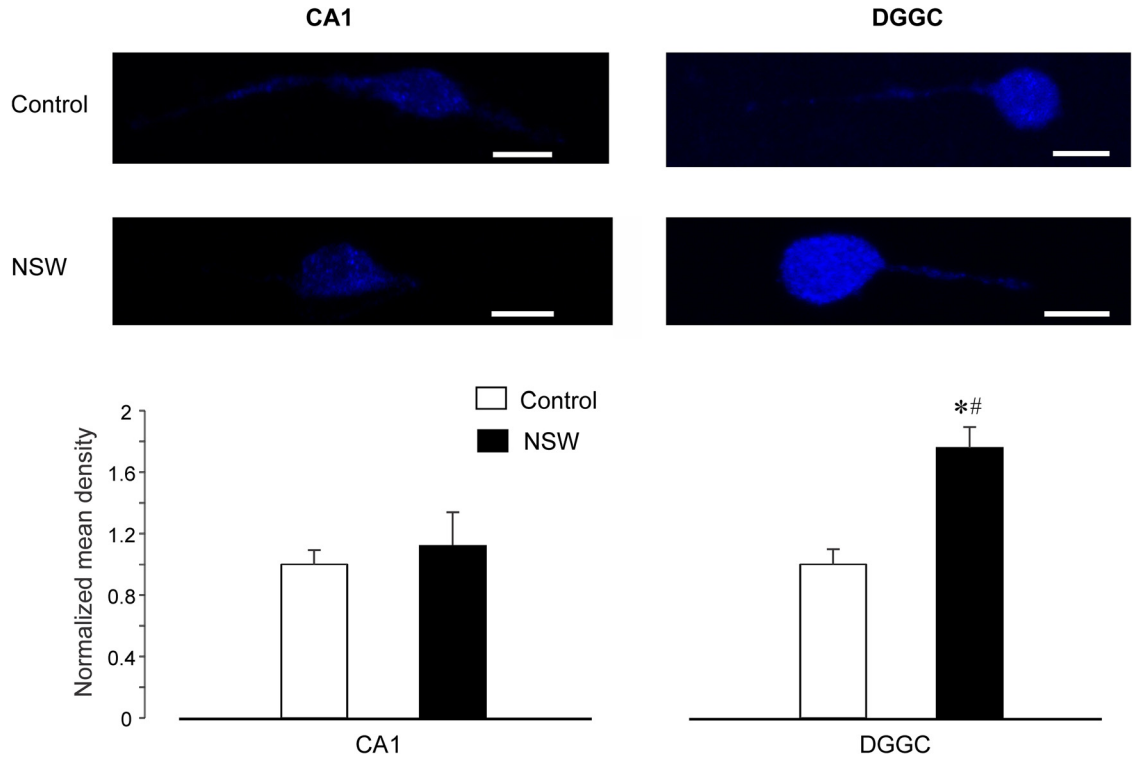

Figure 3. Immunohistochemical distribution of δ subunit in hippocampal CA1 neurons and DGGCs in control and NSW mice. Scale bars, 10 μm. $^*p < 0.05$ versus control; $^\#p < 0.05$ versus CA1 in NSW ($n = 6–24$ cells per group).

with AP. The GABA-A receptor antagonist gabazine (GZ) (50 μM) was applied to the slice perfusion to block phasic and tonic currents. Tonic current was measured as the shift in mean conductance before and after GZ application as demonstrated previously (Wu et al., 2013). Figure 5 depicts modulation of tonic current in granule cells during NSW. Sample traces of tonic current recordings in DGGCs from control and NSW mice were illustrated in Figure 5*A*. Endogenous tonic current was measured in the absence of GABA in the bath perfusion. Control DGGCs displayed significantly greater endogenous tonic current than NSW ($p = 0.0468$, $n = 7–8$ cells per group; Fig. 5*C*). We subsequently measured tonic current with perfusion of 0.3, 1, or 3 μM GABA for a comparative profile of GABA binding of extrasynaptic receptors (Fig. 5*C*). Both 0.3 μM ($p = 0.0398$) and 1 μM ($p = 0.0480$) GABA elicited greater tonic current in NSW than control DGGCs ($n = 5–6$ cells per group and concentration). In response to 1 μM GABA plus 100 nM AP or 1 μM GABA plus 300 nM AP, NSW DGGCs experienced significantly greater enhancement of tonic current than control DGGCs (100 nM AP, $p = 0.0088$; 300 nM AP, $p = 0.0167$; $n = 8–10$ cells per group; Fig. 5*D*).

We measured the RMS channel conductance during each drug application of current recording. Endogenous RMS noise was significantly greater in control (4.0 ± 0.2 pA) than NSW (3.4 ± 0.1 pA) tonic recordings ($p = 0.0274$; $n = 6–7$ cells per group), but 1 μM GABA RMS noise was not significantly different between NSW (3.9 ± 0.1 pA) and control (4.2 ± 0.2 pA; $p = 0.1567$; $n = 8–12$ cells per group). AP significantly increased the RMS noise compared with 1 μM GABA baseline, similar to our previous report (Wu et al., 2013). AP at 300 nM modulated RMS noise to 5.6 ± 0.3 and 6.3 ± 0.4 pA in control and NSW DGGCs, respectively, but this was not significantly different between conditions ($p = 0.1833$). GZ application reduced the RMS noise in a withdrawal-dependent manner. GZ produced a greater reduction of AP-modulated RMS in NSW compared with control at 100 nM AP (Δ−0.9 ± 0.2 pA control vs Δ−1.9 ± 0.2 pA NSW; $p = 0.0030$; $n = 8–10$ cells per group), as well as during 300 nM AP (Δ−2.3 ± 0.3 pA control vs Δ−3.4 ± 0.3 pA NSW; $p = 0.0208$; $n = 8$ cells per group). These results demonstrate the specificity of GABAergic tonic currents in DGGCs.

We explored THIP modulation of tonic current because of its high affinity and efficacy for δ-subunit extrasynaptic receptors (Mortensen et al., 2010; Meera et al., 2011) and different binding site than the allosteric site of neurosteroids (Brown et al., 2002; Stórustovu and Ebert, 2006). THIP acts like a "super agonist" at extrasynaptic receptors (Brown et al., 2002), and its greater efficacy compared with GABA is mostly based on peak response rather than at steady state (Bright et al., 2011). THIP and GABA compete for the same binding site, but the apparent affinity of extrasynaptic receptors for GABA is much higher. Nevertheless, the ability of THIP to enhance tonic inhibition makes it a suitable tool to study extrasynaptic receptor plasticity. In our studies, THIP was applied in an environment without exogenous GABA in the perfusion to allow for high $GABA_AR$ occupancy. A concentration-dependent response was examined for tonic current modulation by THIP in the range 0.03–1 μM, selective for δ-subunit binding (Fig. 5*F*). Tonic currents of NSW DGGCs displayed significantly greater sensitivity to THIP at 0.1 and 0.3 μM concentrations than control DGGCs ($p < 0.05$; $n = 4–6$ cells per group and concentration). We observed desensitization of extrasynaptic current at 1 μM THIP (Fig. 5*E*). Although it is possible that 1 μM THIP is beyond δ-subunit selectivity, it was of note that extrasynaptic desensitization to THIP was more pronounced in NSW native DGGCs (Brown et al., 2002; Bright et al., 2011; Pandit et al., 2013). Previous studies describe that, under steady-state conditions, THIP does not display super-agonist properties (Houston et al., 2012). Therefore, we measured peak

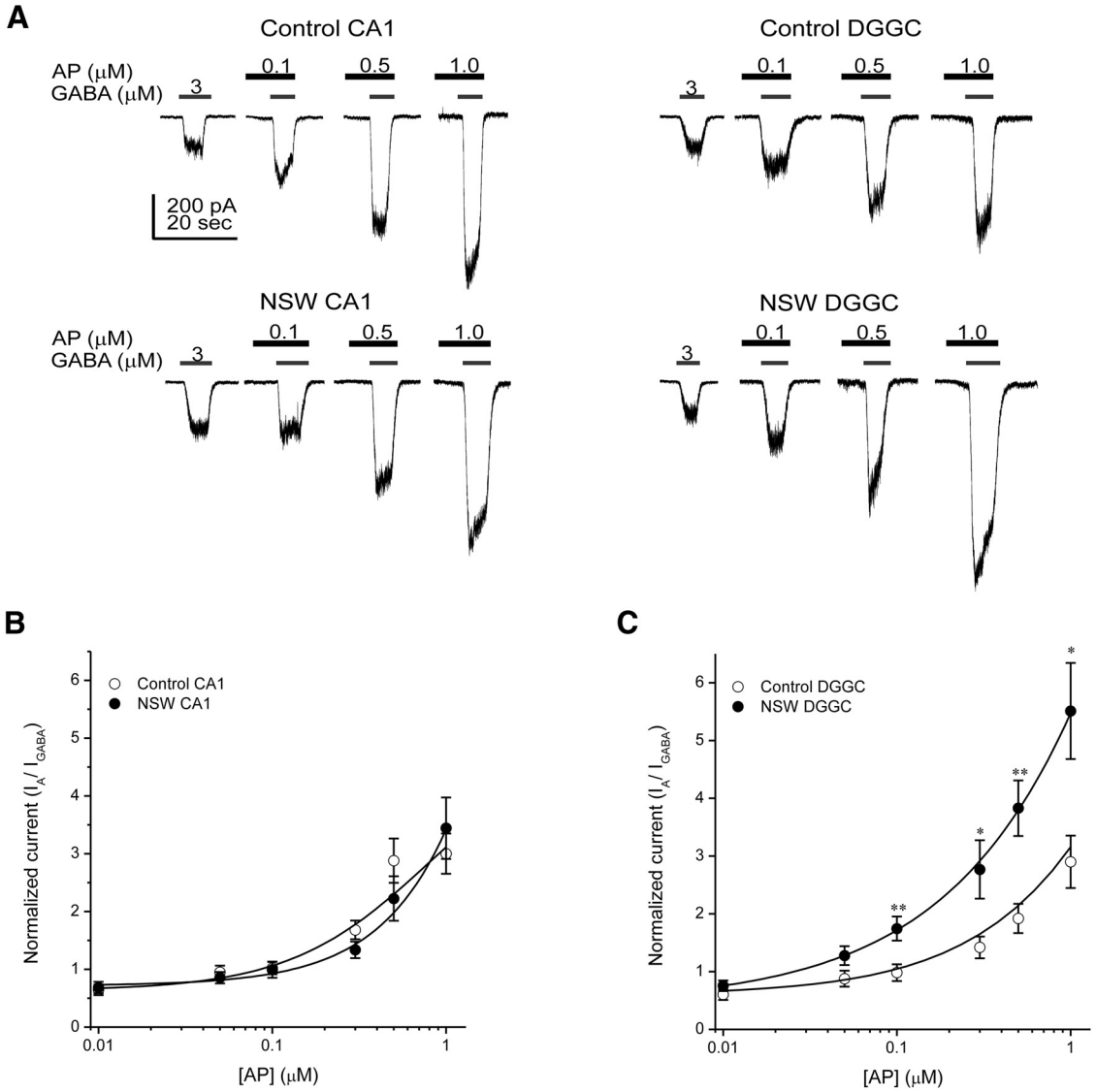

Figure 4. NSW enhances pharmacological sensitivity to AP through allosteric potentiation of GABA-gated currents in dissociated DGGCs but not CA1 neurons. ***A***, Representative whole-cell current recordings of CA1PCs and DGGCs in the NSW paradigm. Neurons displayed concentration-dependent responses to AP potentiation of 3 μM GABA (EC_{10}). ***B***, ***C***, Averaged concentration–response curves for fold potentiation of AP (0.01–1.0 μM), normalized to baseline GABA EC_{10} (I_A/I_{GABA}). Potentiation was averaged for cells of similar condition and concentration after normalization to GABA response. NSW DGGCs displayed greater positive potentiation of GABAergic current by AP. Recordings in whole-cell mode, voltage clamped at −70 mV. Data values represent mean ± SEM. *$p < 0.05$; **$p < 0.01$ versus control ($n = 8$–16 cells per condition and drug concentration).

tonic current 30 s after THIP administration, and we also measured tonic current at the time in which THIP-modulated conductance reached tonic desensitization. The criterion for determining the tonic desensitization is described in Materials and Methods. GZ (50 μM) was applied after 2 min of recording to determine the total tonic current shift. We then compared the difference in peak and desensitized currents between control and NSW DGGCs (Fig. 5*E*,*F*). The peak tonic current for 0.1–1 μM THIP was significantly different between control and NSW ($p = 0.0051$). NSW, but not control, DGGCs displayed significant desensitization compared with the peak current induced by 1 μM THIP ($p = 0.0238$). The percentage change of THIP-dependent current desensitization was significantly different between control (27.5 ± 5.5%) and NSW (50.8 ± 4.7%; $p = 0.0229$; $n = 5$ cells per group) DGGCs. Together, these electrophysiology studies indicate that NSW confers greater sensitivity of extrasynaptic tonic currents to AP and the δ-specific agent THIP within DGGCs.

NSW does not confer enhanced extrasynaptic function in CA1 pyramidal neurons

We observed a modest increase in δ subunit in CA1 and CA3 subfields after NSW (Fig. 2*B*). Previous models of NSW have also suggested that an increase to δ-subunit expression occurs in CA1PCs (Sundstrom-Poromaa et al., 2002; Smith et al., 2007). There is a lack of definitive evidence that increases to δ-subunit expression within hippocampus promote functional, extrasynaptic current within CA1 or CA3 pyramidal cells. To determine whether functional δ-containing extrasynaptic $GABA_AR$ is increased, we measured tonic currents and its modulation by THIP in CA1PCs from NSW mice. Sample traces of tonic current recordings in CA1 from control and NSW mice were illustrated in Figure 5*B*. There were no significant differences to THIP-induced tonic currents in CA1 cells between control and NSW mice (Fig. 5*F*). Unlike DGGCs that exhibited enhanced sensitivity and desensitization to THIP responses, we did not observe significant

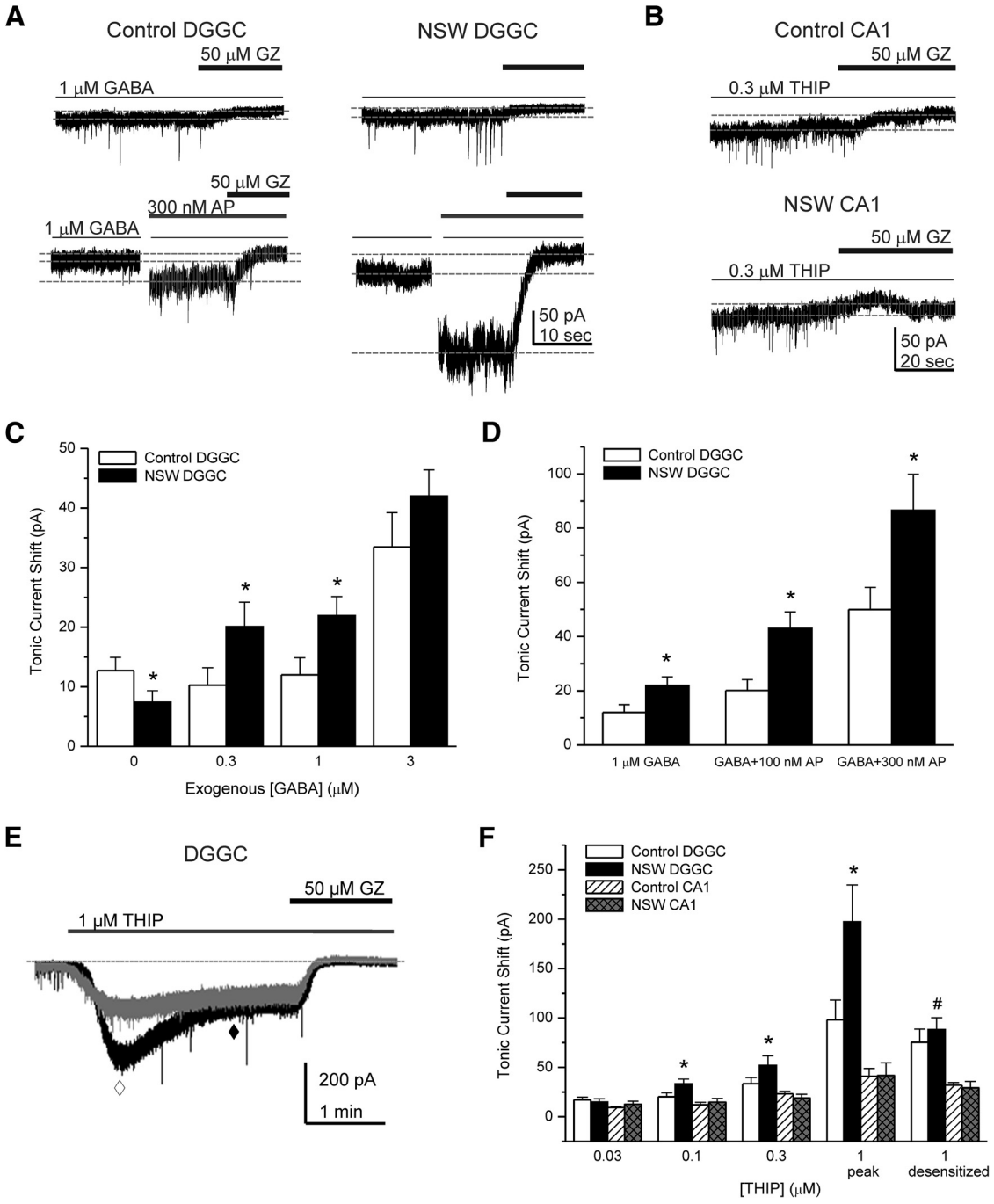

Figure 5. NSW enhances AP potentiation and THIP modulation of tonic currents in DGGCs in hippocampus slices. ***A***, Representative GABAergic tonic current recordings from DGGCs (between 1st and 2nd gray dash lines). AP at 300 nM produced an additional negative shift (between 2nd and 3rd gray dash lines; bottom traces) in the holding current level, and the competitive antagonist GZ at 50 μM produced a positive shift in the holding level, blocking both phasic and tonic currents. Tonic current shift (picoamperes) was measured as the total current change before and after GZ application. The first gray dotted line in each raw trace represents the mean holding current during GZ application. ***B***, Representative GABAergic tonic current recordings from CA1PCs in response to 0.3 μM THIP in NSW mice. ***C***, Concentration response of DGGC tonic current to GABA. Endogenous tonic current (no exogenous GABA) shift was greater in the control condition than NSW; however, NSW DGGCs displayed greater tonic current at 0.3 and 1 μM GABA than control. ***D***, NSW DGGC tonic currents were more sensitive to modulation by AP than control at 100 and 300 nM AP potentiation of 1 μM GABA. ***E***, Representative tonic current recordings from control DGGCs (gray trace) and NSW DGGCs (black trace) attributed to 1 μM THIP application. ***F***, Quantification of tonic current during 0.03–1 μM THIP from CA1PCs and DGGCs. THIP administration at 1 μM at peak (◇ in ***E***) and desensitized (◆ in ***E***) tonic levels from DGGCs were also compared. NSW DGGCs displayed significant desensitization compared with the peak current induced by THIP, whereas control DGGCs did not have significant THIP-induced desensitization of tonic current. In addition, NSW produced a larger percentage change of tonic current than control. CA1PCs did not display such differences in THIP responses after NSW. Recordings in whole-cell mode, voltage clamped at −65 mV. Data values represent mean ± SEM. $^*p < 0.05$ versus control DGGC current; $^{\#}p < 0.05$ versus 1 μM THIP peak current, NSW DGGC ($n = 4–10$ cells for each group and concentration).

desensitization of tonic currents in CA1 at 1 μM THIP (Fig. 5*F*). Overall, these results indicate that δ-subunit upregulation is functionally more significant to the granule cells of the DG and not to CA1PCs.

NSW does not confer enhanced AP sensitivity in δKO mice

To further confirm whether the NSW-induced increase in neurosteroid sensitivity is attributable to extrasynaptic δ-subunit $GABA_A$Rs, we used knock-out mice that lack expression of

δ-containing receptors in the brain as a robust genetic model. Neurons were acutely dissociated from δKO female mice treated in the perimenstrual-like withdrawal paradigm. Voltage-clamp recordings were obtained from DGGC neurons in response to AP coapplied with 3 μM GABA (Fig. 6*A*), similar to the experiments performed in Figure 4. A concentration–response curve was derived for AP potentiation of GABAergic current (Fig. 6*B*), and fractional current responses of AP were compared between NSW and vehicle-injected control δKO animals. In δKO granule cells, AP (0.05–0.30 μM) and GABA produced less modulation of $GABA_A$R currents than that of GABA alone. NSW and control DGGCs from δKO mice displayed no significant differences at any of the concentrations tested (n = 8–12 cells per each group and drug concentration). In addition, modulation by AP was significantly lower in δKO DGGCs than in WT DGGCs.

We acquired tonic current recordings from δKO DGGCs to ascertain the degree of AP sensitivity in a hippocampal network lacking δ subunit (Fig. 6*C*,*D*). Changes to tonic current, RMS, and enhanced AP sensitivity were not evident in δKO animals subjected to withdrawal. Tonic currents were highly attenuated, and control and NSW knock-outs displayed no significant differences in 1 μM GABA (p = 0.8860; n = 5 cells per group) or 1 μM GABA and 300 nM AP (p = 0.9064; n = 6 cells per group). We also examined tonic current attributed to THIP within knock-out DGGCs. THIP did not enhance tonic current in DGGCs from either control or withdrawn mice (data not shown). Overall, these results indicate a lack of NSW-induced function in δKO animals. The neurosteroid sensitivity present in withdrawn mice is attenuated when the δ subunit is genetically and functionally removed from the hippocampus, disallowing plastic increase in δ expression.

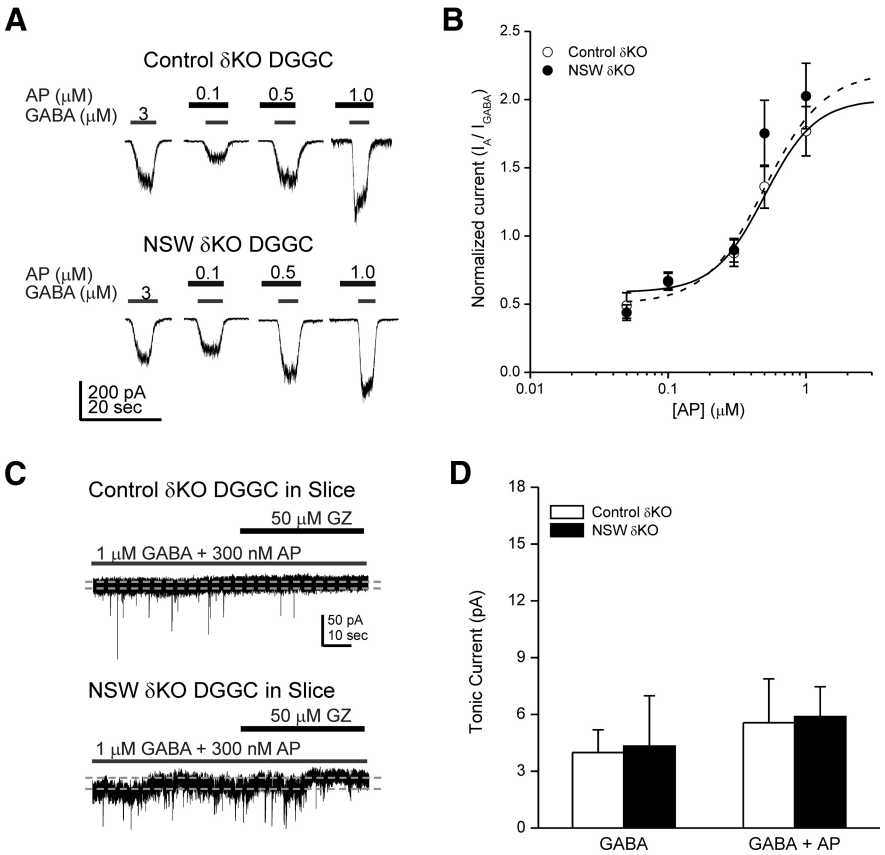

Figure 6. AP sensitivity is attenuated in δKO mice undergoing NSW. ***A***, Representative whole-cell current recordings of dissociated DGGCs from δKO mice. ***B***, Concentration–response curve of δKO DGGCs attributed to AP modulation of GABA-gated current (I_A/I_{GABA}). AP potentiation of current was not significantly different between control and NSW DGGCs at any of the AP concentration tested (0.05–1 μM). ***C***, Representative tonic current recordings from control and NSW DGGCs in hippocampus slices from δKO female mice. The gray dotted line represents the mean holding current during GZ application. GZ at 50 μM antagonized phasic $GABA_A$R currents but caused little to no shift in the tonic current holding level of δKO neurons. ***D***, Tonic current shift attributed to GZ is reduced and minimal in δKO DGGCs in control and NSW conditions. There were no significant differences in tonic current between NSW and control DGGCs during 1 μM GABA or during 1 μM GABA plus 300 nM AP application. Data represent mean ± SEM (n = 5–12 cells). Recordings in whole-cell mode, voltage clamped at −70 mV (***A***, ***B***) or −65 mV (***C***, ***D***).

NSW influences the amplitude and kinetics of mIPSCs of $GABA_A$Rs

To determine the extent of withdrawal-induced modulation by AP on synaptic receptors, GABAergic mIPSCs were recorded in DGGCs from brain slices in the presence of 0.5 μM TTX in perfusion and 5 mM QX-314 in the recording electrode pipette. The properties of amplitude, 10–90% rise time, decay time constants, and interevent interval (as a measure of frequency) were analyzed from mIPSCs (Fig. 7; Table 1). The average mIPSC from each neuron was best fit with a double-exponential decay curve, depicted as τ_1 and τ_2. A weighted decay constant, τ_w, was also determined (see Materials and Methods). mIPSC frequency is related to functional number of synapse release sites and the rate of presynaptic release (Cherubini and Conti, 2001). $GABA_A$R channel kinetics are highly influenced by receptor subunit composition (Smith and Gong, 2005; Smith et al., 2007; Carver et al., 2013). Postsynaptic receptor density, synaptic vesicle GABA content, and dendritic cable properties contribute to mIPSC amplitude (Nusser et al., 1997; Cherubini and Conti, 2001). We hypothesized that NSW would not alter presynaptic GABA release properties; however, we proposed that NSW-induced sensitivity of AP may affect postsynaptic current and kinetics attributed to the α4 and δ subunit expressional changes (Fig. 7). Within recordings of endogenous (no GABA) or 1 μM GABA perfusion, the amplitude, kinetics, and frequency were not significantly different between withdrawal and control DGGCs (Table 1). These experiments were repeated with 1 μM TTX to ensure that the recorded IPSCs were action potential independent. There were no significant differences in amplitude, decay constants, and frequency of mIPSCs when comparing 0.5 and 1.0 μM TTX. In the addition of 300 nM AP, peak amplitude was significantly greater in withdrawal than control DGGCs (p = 0.0046; n = 5 cells per group). Neurosteroids, such as AP, increase the channel opening probability of $GABA_A$Rs and prolong the decay kinetics (Carver and Reddy, 2013). The τ_w constant derived from τ_1 and τ_2 time constants of phasic $GABA_A$Rs from DGGCs was consistent with previous reports (Sun et al., 2007). AP (300 nM) resulted in a significant increase in τ_2 and τ_w decay time constants of both control and NSW (p = 0.0011 vs control 1 μM GABA; p <

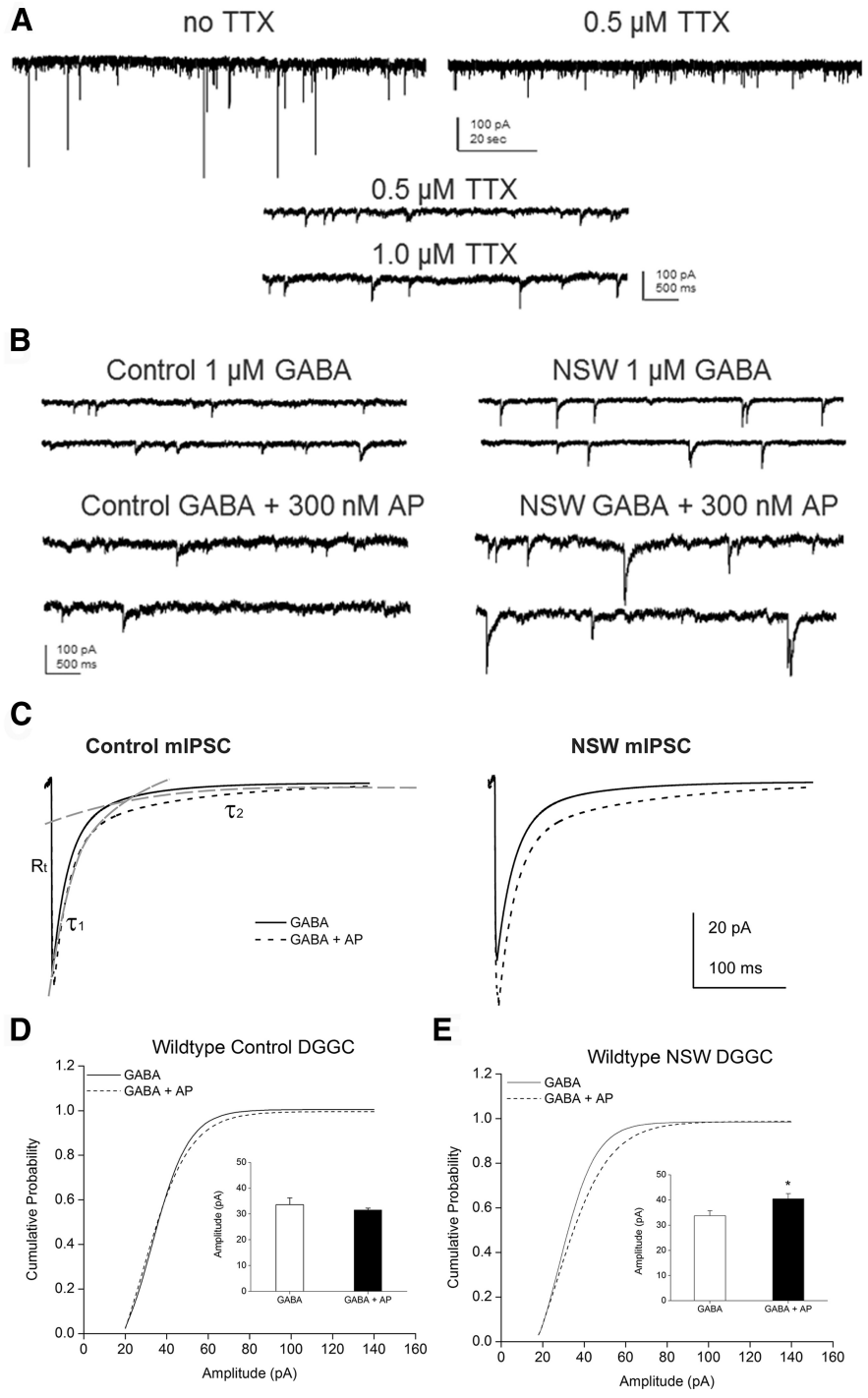

Figure 7. mIPSCs are sensitive to AP in mice undergoing NSW. Phasic events were recorded from patch-clamped DGGCs in hippocampus slices. $GABA_A$R synaptic activity was isolated using TTX, APV, and DNQX. Synaptic current was blocked with the addition of bicuculline (10 μM) or GZ (50 μM). ***A***, Representative traces of IPSCs before and after TTX application and mIPSCs in 0.5 or 1.0 μM TTX. ***B***, mIPSC recordings during GABA and AP modulation. Note the increased RMS channel noise during AP drug application. ***C***, Averaged mIPSC events recorded from control and NSW DGGCs in the presence of 1 μM GABA (solid line) or 1 μM GABA coapplied with 300 nM AP (dashed line) and biexponential fitted for fast and slow decay time constants, τ_1 and τ_2 (gray dash lines), respectively. NSW DGGCs displayed significantly greater amplitude ($p = 0.0046$) and τ_2 decay ($p = 0.0011$) during application of 300 nM AP than control DGGCs ($n = 5$–10 cells per group; R_t, downward rise time; Table 1). Cumulative probability curves for WT control (***D***) and NSW (***E***) mIPSC amplitude, plotted from all events. The Kolmogorov–Smirnov test was used to compare mIPSCs before and after application of AP in DGGCs ($n = 5$–10 per group). ***D***, ***E***, ***Insets***, Mean peak amplitude of mIPSCs. *$p < 0.05$ vs GABA. Recordings in whole-cell mode, voltage clamped at −65 mV.

0.0001 vs NSW 1 μM GABA). Whereas the control mIPSCs exhibited an average 62.1 ± 6.0% increase to τ_2 decay during AP modulation, the NSW mIPSCs exhibited an average 135.8 ± 5.2% increase to τ_2 decay. Control mIPSCs had an average of 33.1 ± 5.5% increase to τ_w decay during AP modulation, and NSW mIPSCs had an average 66.8 ± 6.3% increase to τ_w decay. This difference in mean percentage change of τ_2 and τ_w was statistically significant between the control and NSW groups ($p < 0.0001$ for τ_2, $p = 0.0008$ for τ_w). Data represent mean values for 5–10 cells per group and application.

To determine whether the NSW-induced changes to synaptic activity we observed are related to δ-subunit expression, we recorded mIPSCs from δKO mice subjected to the withdrawal paradigm. AP did not significantly prolong the decay in δKOs as that occurred in WT neurons, and there were no significant differences in mIPSC properties between control and withdrawal in knock-out DGGCs (Table 1). In addition, during AP administration, δKO mIPSCs displayed faster τ_2 and τ_w decay than WT mIPSCs in both control and withdrawal conditions.

We found that AP has a greater effect on prolongation of mIPSC decay in DGCCs from NSW mice, an effect prevented by δKO (Table 1), which indicates that δ-containing $GABA_A$Rs mediate this effect. NSW-induced changes in phasic decay kinetics did not occur with 1 μM GABA alone. However, NSW tonic currents displayed greater sensitivity to 1 μM GABA. This difference in activity may represent distinct receptor subtype compositions and their GABA-gating properties within the native neuronal population (Mortensen et al., 2010). Our results shows that AP is able to alter the efficacy state and channel opening of the phasic-responding receptors in withdrawn animals under the above control conditions. It is possible that a perisynaptic population of $GABA_A$Rs could respond to synaptic spillover of GABA during upregulated δ expression (Bianchi and Macdonald, 2003). However, there is evidence that suggests that δ-containing receptors are relatively insensitive to phasic GABA activation that could occur through synaptic spillover (Bright et al., 2011).

Because low, ambient GABA (1 μM) was unable to elicit a significant difference in the phasic current, we further explored mIPSCs with higher concentrations of exogenous GABA to engender a condition of higher-efficacy synaptic response. GABA concentrations of 3 and 10 μM were suffi-

Table 1. $GABA_A$ receptor-mediated mIPSC characteristics in control and NSW mice

Group (*n*)	Amplitude (pA)	$Rise_{10-90\%}$ (ms)[a]	Decay τ_1 (ms)[a]	Decay τ_2 (ms)[a]	Decay τ_w (ms)	IEI (s)
WT control endogenous						
0.5 μM TTX (5)	30.8 ± 1.6	1.2 ± 0.2	12.6 ± 0.8	51.6 ± 3.9	27.2 ± 1.5	1.4 ± 0.1
1.0 μM TTX (5)	27.3 ± 2.4	1.1 ± 0.2	10.2 ± 0.6	48.5 ± 5.8	25.2 ± 2.9	1.6 ± 0.1
WT NSW endogenous						
0.5 μM TTX (5)	30.3 ± 1.9	1.0 ± 0.1	11.5 ± 1.3	49.2 ± 5.5	25.3 ± 1.1	1.1 ± 0.2
1.0 μM TTX (5)	32.7 ± 1.4	0.9 ± 0.1	13.9 ± 1.1	49.0 ± 2.3	26.4 ± 2.8	1.4 ± 0.1
WT control						
+1 μM GABA (10)	33.7 ± 2.6	1.2 ± 0.3	12.4 ± 0.6	49.6 ± 3.3	26.0 ± 0.9	1.6 ± 0.3
+ GABA + 300 nM AP (5)	31.5 ± 0.8	1.4 ± 0.1	12.6 ± 1.8	80.4 ± 8.3*	34.6 ± 1.4*	1.7 ± 0.2
WT NSW						
+ 1 μM GABA (10)	33.8 ± 2.0	1.2 ± 0.2	14.4 ± 1.4	43.3 ± 4.2	25.3 ± 1.9	1.3 ± 0.2
+ GABA + 300 nM AP (5)	40.5 ± 2.1*,**	1.6 ± 0.3	16.5 ± 2.0	102.1 ± 7.9*	42.2 ± 3.1*	1.6 ± 0.3
δKO control						
+ 1 μM GABA (9)	33.7 ± 2.2	1.3 ± 0.1	12.2 ± 0.9	47.8 ± 4.0	26.0 ± 2.6	1.8 ± 0.1
+GABA + 300 nM AP (9)	34.8 ± 1.3	1.5 ± 0.2	15.3 ± 1.4	58.5 ± 5.1***	29.5 ± 1.1***	1.7 ± 0.3
δKO NSW						
+ 1 μM GABA (6)	32.4 ± 2.3	1.1 ± 0.2	11.7 ± 1.8	45.8 ± 6.0	22.5 ± 2.5	1.8 ± 0.6
+ GABA + 300 nM AP (5)	34.9 ± 2.0***	1.0 ± 0.1	10.1 ± 1.0	47.9 ± 7.5***	23.6 ± 2.3***	1.6 ± 0.4

mIPSCs were recorded in the presence of 0.5 μM TTX unless denoted otherwise. Groups denoted as + GABA + 300 nM AP were recorded during perfusion of 1 μM GABA and 300 nM AP. Recordings were from voltage-clamped (−65 mV) DGGCs in hippocampus slices. *$p < 0.05$ versus WT NSW + 1 μM GABA alone; **$p < 0.05$ versus WT control + GABA + 300 nM AP; ***$p < 0.05$ versus WT NSW + GABA + 300 nM AP; independent two-tailed *t* test. IEI, Interevent interval as a measure of frequency. Data values represent mean ± SEM.

[a]Rise time, decay τ_1, and decay τ_2 are represented as R_t, τ_1, and τ_2 in Figure 7*C*. $Rise_{10-90\%}$ represents duration for downward shift 10–90% of the amplitude.

cient to significantly increase the amplitude τ_2 and τ_w decay of mIPSCs from WT control DGGCs (3 μM GABA: amplitude, 44.0 ± 3.0 pA; τ_1, 15.4 ± 2.2 ms; τ_2, 70.9 ± 3.8 ms; τ_w, 34.9 ± 2.3 ms; 10 μM GABA: amplitude, 54.1 ± 5.7 pA; τ_1, 16.5 ± 2.7 ms; τ_2, 109.8 ± 12.0 ms; τ_w, 45.7 ± 6.6 ms; $n = 5–6$ cells per concentration). Compared with 1 μM GABA, WT DGGCs displayed an average 42.9 ± 2.6% increase in τ_2 in 3 μM GABA, whereas DGGCs in 10 μM GABA had an average 121.4 ± 10.2% increase in τ_2. We also explored mIPSCs within δKO DGGCs in response to 3 and 10 μM GABA (3 μM GABA: amplitude, 30.2 ± 1.0 pA; τ_1, 18.6 ± 1.7 ms; τ_2, 57.8 ± 3.1 ms; τ_w, 32.4 ± 1.5 ms; 10 μM GABA: amplitude, 48.9 ± 6.8 pA; τ_1, 15.7 ± 1.5 ms; τ_2, 64.8 ± 5.8 ms; τ_w, 34.3 ± 1.0 ms; $n = 4–5$ cells per concentration). δKO DGGCs had an average 20.9 ± 1.4% change in τ_2 in 3 μM GABA and an average 35.6 ± 3.1% change in τ_2 in response to 10 μM GABA when compared with 1 μM GABA. The difference in τ_2 decay was significantly reduced in δKO DGGCs compared with WT for each GABA concentration ($p < 0.05$), suggesting an increased contribution of δ subunit to phasic currents in control conditions, albeit at supraphysiological concentrations of GABA. These results provide strong evidence that δ-containing receptors require higher-efficacy gating to mediate phasic currents, such as that occurring by neurosteroid potentiation of GABA (Bianchi and Macdonald, 2003). In our model, NSW is sufficient to promote prolongation of synaptic current decay and amplitude in response to AP but not to low (≤1 μM), ambient GABA alone.

NSW causes increased susceptibility to hippocampus kindling seizures

To investigate whether the NSW-induced changes in $GABA_A$Rs mediating tonic inhibition affects neuronal network excitability in a seizure model, we studied the susceptibility of NSW mice to seizures in rapid hippocampus kindling model of epilepsy (Reddy and Mohan, 2011; Wu et al., 2013). Adult female mice were surgically implanted with a bipolar electrode in the hippocampus. After surgery recovery and subsequent withdrawal paradigm, the mice were subjected to rapid kindling stimulations at 125% AD threshold at 30 min intervals until stage 5 seizures were consistently reached. The progression of rate of kindling, electrographic AD threshold, and cumulative AD activity time for kindling criterion were recorded as main indices of epileptogenesis (Fig. 8). Mean rate of kindling was significantly faster in NSW animals (Fig. 8*B*, $p = 0.0098$). Mean AD threshold current was significantly reduced in NSW mice (Fig. 8*C*, $p = 0.0149$). Cumulative AD duration was not significantly different between the control and withdrawal groups (Fig. 8*D*, $p = 0.1384$). The amplitude of AD spike activity was markedly greater in NSW mice than in control mice (data not shown). The rapid kindling experiments were conducted in δKO mice with and without NSW induction. The δKO animals did not display significant differences in any of the seizure parameters between the control and NSW groups (Fig. 8*B–D*). Thus, these results are consistent with the increased excitability and susceptibility of animals undergoing NSW with δ subunit intact, which is a key triggering factor for catamenial seizure exacerbation.

Fully kindled mice undergoing NSW exhibit increased sensitivity to the antiseizure effects of AP

To determine the therapeutic potential of neurosteroids in perimenstrual catamenial epilepsy, we tested the effect of neurosteroid AP on heightened seizures caused by perimenstrual-like NSW in fully kindled mice exhibiting stage 5 seizures. Female WT and δKO mice were subjected to once-daily kindling until they exhibited stage 5 seizures for 3 consecutive days, which is considered the fully kindled state. WT mice reached the fully kindled state with consistent stage 5 seizures after 10–16 stimulations (Fig. 8*B*), as reported previously (Reddy et al., 2012). Fully kindled WT and δKO mice undergoing NSW condition were treated with AP or vehicle injections. Fifteen minutes after AP administration, animals were stimulated at their designated AD threshold. Behavioral seizure stage and electrographic AD duration were evaluated as criteria of drug efficacy for sensitivity assessment (Fig. 9). AP (1–10 mg/kg, s.c.) exerted dose-dependent suppression of the behavioral seizures (Fig. 9*A*) and AD duration (Fig. 9*B*) in WT control (nonwithdrawal) mice. In contrast, after NSW, AP produced greater suppression of behavioral seizures and AD duration in WT mice with significant effects at 1 and 5 mg/kg compared with the control group ($p < 0.01$; $n = 6–9$ mice

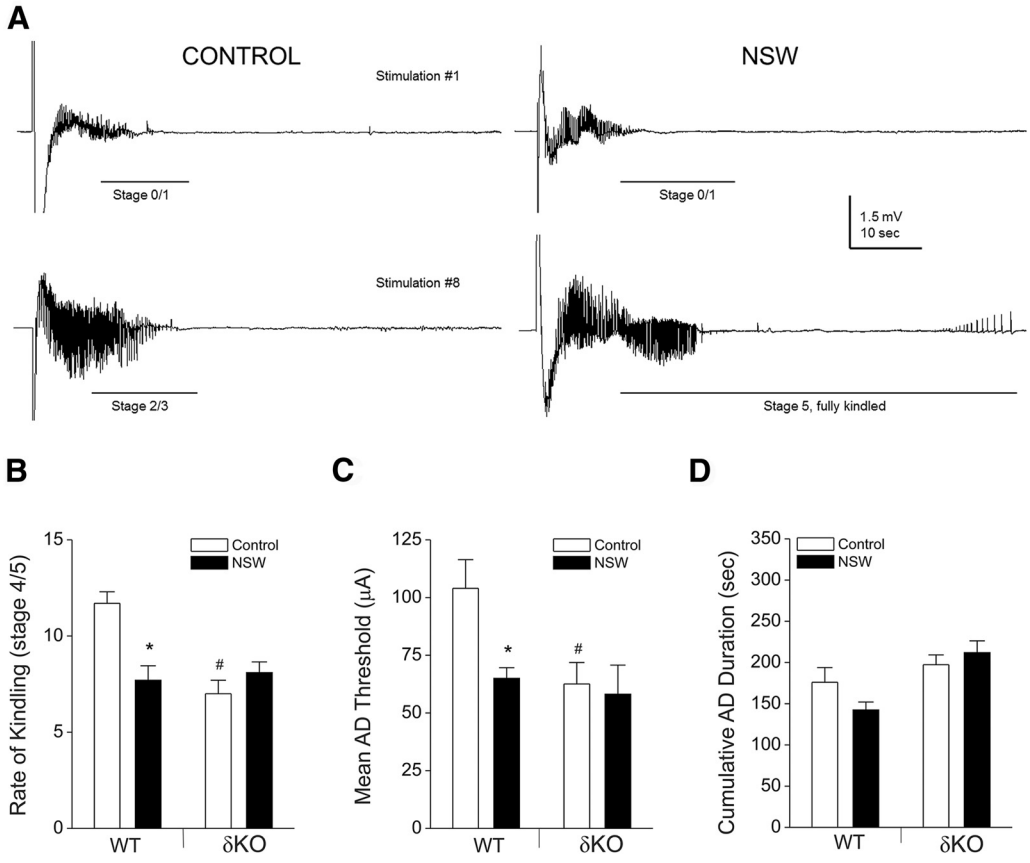

Figure 8. Changes in susceptibility to hippocampus kindling epileptogenesis in NSW WT and δKO mice. Mice were subjected to rapid kindling stimulations at 125% AD threshold at 30 min intervals until consistent display of stage 5 seizures. ***A***, Representative electrographic AD seizure activity recorded immediately after kindling stimulation of the hippocampus, recorded in control and NSW WT mice. The black bar above the stage designation denotes the period of the electrograph in which the animal experienced seizure activity. ***B***, WT mice experiencing NSW developed stage 4/5 seizures in a significantly less number of stimulations than control mice, as denoted by rate of kindling. ***C***, WT mice undergoing NSW mice showed a lower mean AD threshold than control mice, requiring less current stimulation to achieve epileptogenic seizure activity. Control δKO mice exhibited accelerated rapid kindling and had lower AD threshold than WT control counterparts. ***D***, Cumulative AD duration was similar between control and NSW groups. $^*p < 0.05$ versus control of similar genotype; $^{\#}p < 0.05$ versus WT control ($n = 9$–15 animals per group).

per group). These experiments were repeated in fully kindled δKO mice. In contrast to WT counterparts, fully kindled δKO mice undergoing NSW failed to exhibit any significant difference in seizure expression (Fig. 9*C*) and AD duration (Fig. 9*D*) after AP (1–10 mg/kg, s.c.) treatment ($n = 6$–9 mice per group). These results confirm enhanced neurosteroid sensitivity in WT mice attributed to upregulation of δ subunit. However, the time course profiles for onset and duration of seizure expression after AP (10 mg/kg) treatment were similar in WT and δKO mice (Fig. 9*E*,*F*), indicating the lack of significant pharmacokinetic factors in drug sensitivity related to genotype. Moreover, plasma levels of AP achieved at various doses of AP treatment (10 mg/kg) were correlated with seizure protection in WT control and withdrawn groups (Fig. 9*E*,*F*), indicating a linear pharmacokinetic–pharmacodynamic relationship. Overall, the neurosteroid AP produced enhanced antiseizure efficacy (50%) in WT NSW but not δKO NSW animals, confirming the δ-subunit-related enhanced sensitivity to neurosteroids in the NSW model of catamenial epilepsy (Reddy and Rogawski, 2001; Reddy et al., 2012).

Antisense knockdown of δ subunit in WT mice diminishes the NSW-associated enhanced sensitivity to AP

To further investigate whether enhanced neurosteroid sensitivity is attributable to alteration in the abundance of δ subunit in the hippocampus, AP was tested further in fully kindled WT mice with antisense knockdown of δ-subunit expression to selectively block the δ subunit in the brain. Fully kindled mice undergoing NSW were treated with either 5 nmol of δ missense or 5 nmol δ antisense oligos, and seizure studies were performed 24 h after NSW induction. This antisense dosage has been shown previously to markedly reduce δ-subunit protein expression within the hippocampus when compared with missense control (Maguire et al., 2005). AP produced a dose-dependent enhanced suppression of behavioral seizure activity (Fig. 10*A*) and AD duration (Fig. 10*B*) with significant effects at 1 and 10 mg/kg in the NSW missense but not antisense group ($p < 0.01$ vs missense control; $n = 6$–9 mice per group), confirming that the greater AP protection against NSW-induced heightened seizures is dependent on the abundance of δ subunit in the hippocampus. These results are consistent with enhanced neurosteroid sensitivity as observed in other models of NSW (Reddy and Rogawski, 2000, 2001; Reddy et al., 2012).

Discussion

The main finding of this study is perimenstrual-like withdrawal from neurosteroids results in striking increase in extrasynaptic δ-containing $GABA_A$Rs in the DG, a key limbic subregion associated with epilepsy pathology. Upregulation of δ subunit confers increased sensitivity to AP potentiation of $GABA_A$R-mediated tonic inhibition in DGGCs. The prominent increase in δ-subunit expression specific to the DG exemplifies its "gate-keeping" function in controlling baseline inhibition and network inputs in the

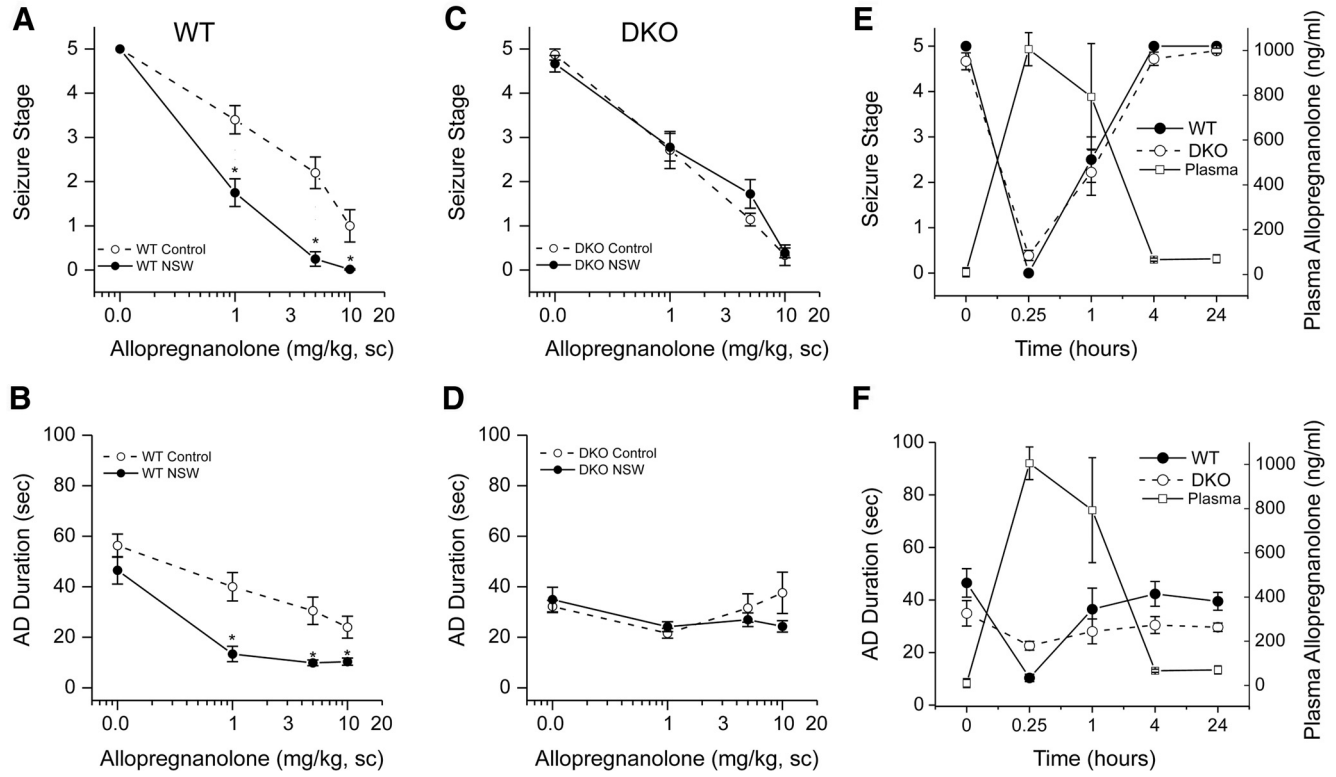

Figure 9. NSW confers enhanced antiseizure effects to AP in fully kindled WT but not δKO (DKO) mice. Fully kindled mice undergoing NSW were used for testing the effect of AP on seizure activity. Dose–response curves for AP-induced (1–10 mg/kg, s.c.) suppression of behavioral seizure stage (***A***) and AD duration (***B***) in WT mice. Dose–response curves for AP-induced (1–10 mg/kg, s.c.) suppression of behavioral seizure stage (***C***) and AD duration (***D***) in δKO mice. There were no significant differences between δKO control and NSW seizure modification by AP. Time course correlation between plasma AP levels and seizure stage (***E***) and AD duration (***F***) in WT and δKO mice. Vehicle or AP was injected 15 min before kindling stimulations or plasma sample collection. Values represent mean ± SEM. ***A–D***, $^*p < 0.05$ versus control ($n = 6$–9 animals per group).

hippocampus (Coulter and Carlson, 2007). These findings provide a molecular mechanism for enhanced anticonvulsant activity of neurosteroids in perimenstrual models of catamenial epilepsy and thereby strengthen the rationale for neurosteroid therapy of catamenial epilepsy.

We observed significant upregulation of δ-subunit expression in the hippocampus during perimenstrual-like NSW, confirming the role of extrasynaptic $GABA_A$Rs in response to fluctuating neurosteroid levels in the brain. This novel observation is consistent with the ovarian cycle-linked regulation of the plasticity and function of extrasynaptic $GABA_A$Rs (Reddy et al., 2012; Wu et al., 2013). Although other regions within the hippocampus had marginally increased expression of δ subunit, the withdrawal-induced δ levels and membrane surface insertion were directed most significantly within the DG. This in turn resulted in functional increases to neurosteroid potentiation of extrasynaptic receptors. Previous reports of NSW-induced upregulation of $GABA_A$Rs have focused on expressional changes within CA1 pyramidal neurons (Smith et al., 2007, 1998a,b; Sundstrom-Poromaa et al., 2002). A NSW-induced increase to δ subunit has not been shown previously within the DG. Our findings of δ-specific perimenstrual upregulation in DGGCs confirm a functional role for $\alpha4\beta\delta$ receptors in modulating excitability in catamenial epilepsy.

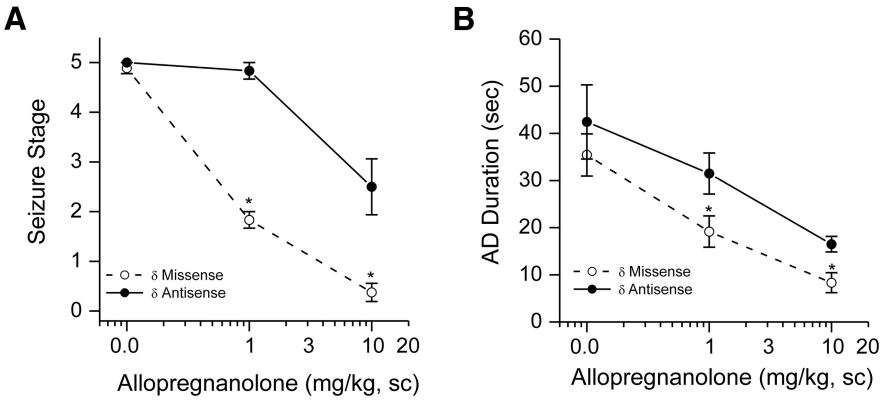

Figure 10. Antisense knockdown of $GABA_A$R δ subunit prevents the NSW-induced enhanced AP sensitivity in protecting against kindling-induced seizures. Fully kindled mice received either δ missense or δ antisense oligos after induction of NSW. AP (1 and 10 mg/kg) inhibition of behavioral seizures (***A***) and AD duration (***B***) was significantly decreased in mice after intracerebroventricular administration of δ antisense but not δ missense oligos on day 7 of the withdrawal protocol (Fig. 1). $^*p < 0.01$ versus the antisense group. Data values represent mean ± SEM ($n = 6$–9 animals per group and dose).

The mechanisms underlying perimenstrual δ-subunit plasticity remain unclear. The early growth response factor-3 pathway is implicated in NSW-induced α4 subunit upregulation, and this has been found to occur independently of any PR interaction (Gangisetty and Reddy, 2010). The upregulation of δ subunit was also evident in PRKO mice experiencing NSW. Thus, it is likely that the δ-subunit plasticity is neurosteroid dependent and not attributed to PR activation by progesterone in the perimenstrual model. It is likely that cellular machinery involved in protein and

receptor trafficking may have an important role in the expression of $GABA_AR$ subunits (Jacob et al. 2008).

In this study, AP was used as a prototype neurosteroid to study the function of $GABA_ARs$ in the perimenstrual model. Other neurosteroids could have a role in modulating neuronal excitability (Tuveri et al., 2008; Reddy and Ramanathan, 2012), but the clear correlation between cyclic progesterone and perimenstrual seizure susceptibility led us to hypothesize that NSW and subsequent sensitivity to AP is strongly mediated by δ-containing receptors (Reddy, 2009). Finasteride inhibition of 5α-reductase results in decreased AP synthesis in mice (Reddy et al., 2012). This directed decline in AP was used to determine the basis for neurosteroid sensitivity similar to that occurring in women experiencing perimenstrual withdrawal.

Consistent with previous studies of α4,δ-containing, recombinant receptors (Brown et al., 2002), our findings in native DGGCs indicate a significant increase in receptor function by AP in the withdrawal model. Physiological concentrations of AP (100–300 nM) produced significantly greater $GABA_AR$ current modulation in NSW compared with control mice (Fig. 4). Furthermore, δKO DGGCs did not display enhanced sensitivity to AP during withdrawal, suggesting that NSW-induced functional changes are δ directed. This demonstrates a key role by extrasynaptic, δ-containing receptors in response to endogenous neurosteroids in the DG during withdrawal despite a pathological susceptibility to seizures (Stell et al., 2003).

The upregulation of δ subunit was substantial enough to allow for a detectable change in AP potentiation of whole-cell $GABA_AR$ current in DGGCs but not in CA1PCs. Although we observed significant increases to δ-subunit expression in CA1, this did not result in increased AP potentiation of $GABA_AR$ current within these neurons. It has been reported previously that δ-containing receptors do not contribute to neurosteroid sensitivity or inhibitory tonic current within the CA1 (Stell et al., 2003; Glykys et al., 2008). Within male mice under control conditions, tonic inhibition in CA1 neurons is mediated primarily by α5βγ2 receptors (Glykys et al., 2008). We found that NSW does not confer functional increases to extrasynaptic current in CA1, as demonstrated with δ-sensitive agents (Fig. 5*B*,*F*). Membrane surface expression of δ-containing receptors is profuse within the DG but is sparse within the CA1, CA2, and CA3 regions (Pirker et al., 2000; Peng et al., 2002). We reported previously that the estrous cycle-dependent δ-subunit plasticity and function were specific to DG and not to CA1 neurons (Wu et al., 2013). The large difference in AP modulation between DGGC and CA1 neurons suggests region-specific plasticity of $GABA_ARs$ and neurosteroid sensitivity in this perimenstrual-like model of catamenial epilepsy.

In the NSW model, we investigated the tonic current function of extrasynaptic $GABA_ARs$ in DGGCs. Low, extracellular GABA (0.3–1.0 μM) produced greater tonic current in the NSW condition than control. The AP potentiation of tonic current in withdrawal DGGCs was also significantly greater than control DGGCs. Within δKO DGGCs, the substantial reduction of tonic current typical for the knock-out model did not revert to higher levels during NSW, confirming that withdrawal-associated potentiation of tonic current is δ mediated. We also explored THIP modulation of tonic current and found that NSW DGGCs had enhanced tonic current at THIP concentrations reported to be δ-subunit selective (Meera et al., 2011). These findings signify enhancement of neurosteroid sensitivity to promote extrasynaptic receptor function and defines a functional role of δ-sensitive agents to modify network inhibition of the hippocampus.

Upregulation of δ-subunit expression may affect postsynaptic function. In the NSW model, $GABA_AR$ mIPSC properties were unaltered in DGGCs. However, in response to AP, mIPSCs displayed increased amplitude and prolonged decay kinetics. We did not observe any similar AP-sensitivity changes to mIPSC properties in the δKO mouse during withdrawal. In fact, decay kinetics were modestly reduced in δKO DGGCs during AP administration (Table 1). Therefore, withdrawal-induced increases in δ levels confer higher synaptic sensitivity to neurosteroids. Our findings are consistent with previous reports of AP-modulated changes in postsynaptic function (Sun et al., 2007). Our results show that AP only potentiated mIPSC amplitude from NSW but not from control cells. Neurosteroids prolong the kinetics of synaptic $GABA_AR$ channels, resulting from longer channel gating time in open configuration (Bianchi and Macdonald, 2003). Because of heightened neurosteroid sensitivity in NSW, there is preferential enhancement of the low-efficacy state during neurosteroid binding, thereby contributing to the AP-sensitive phasic currents gated by GABA. We found this modulation of phasic current to be neurosteroid and δ-subunit dependent. mIPSCs from δKO mice DGGCs have a faster decay time constant (Mihalek et al., 1999), and neurosteroid modulation of synaptic currents is reduced (Spigelman et al., 2003). We did not detect changes to subunits in the hippocampus primarily assembled at the synapse (α1, α2, β2, γ2). Therefore, it is unlikely that the increase of α4 and δ subunits promotes compensational changes to other subunits in the withdrawal model. Moreover, previous studies suggest that α4βγ2 receptors exhibit faster desensitization than α4βδ but exhibit slower decay kinetics (Brown et al., 2002; Smith and Gong, 2005). Overall, these results expand on previous findings by presenting a novel model in which strong δ upregulation promotes neurosteroid sensitivity on phasic receptors.

Despite increased awareness of neurosteroids, the molecular pathophysiology of catamenial epilepsy remains unclear. A decline in neurosteroid in the brain and subsequent reduction of $GABA_AR$-mediated inhibition can create an environment of hyperexcitability within the limbic network. Mice that experience inhibition of AP synthesis show enhanced susceptibility to limbic epileptogenesis (Reddy, 2009; Reddy et al., 2012). We induced NSW in an *in vivo* rapid kindling paradigm to explore acute epileptogenesis during the dynamic $GABA_AR$ plasticity. Despite upregulation of extrasynaptic receptors, WT mice undergoing NSW experienced heightened seizure susceptibility. This could be attributed to the lack of modulatory control of inhibition following imbalance of GABA and glutamate neurotransmitters during kindling (Minamoto et al., 1992). In limbic epilepsy, tonic inhibition mediated by δ-containing receptors remains intact; moreover, GABA uptake by transport proteins also retains function (Pavlov et al., 2011; Pavlov and Walker, 2013), preventing accumulation of extracellular GABA that could increase inhibitory gain. Our reported decrease in endogenous tonic current during NSW suggests that extrasynaptic receptors experience less inhibitory modulation attributed to the altered hormonal environment. Pathophysiological mechanisms and network aberrations may constrain $GABA_AR$ function in epilepsy (Cohen et al., 2003). The rapid kindling of the hippocampus in NSW mice produced an accelerated progression of epileptogenesis, as well as development of sustained, excitable electrical activity that originated within the hippocampus. These results suggest that the hippocampus is more susceptible to excitability attributed to diminished AP. Fully kindled mice undergoing NSW displayed enhanced antiseizure sensitivity to the neurosteroid AP (Fig. 9*A*,*B*), and lack of δ subunit or antisense knockdown of δ subunit di-

minished such enhanced neurosteroid sensitivity (Figs. 9*C*,*D*, 10). Therefore, plastic increase in δ-containing $GABA_A$Rs with high affinity for neurosteroids provides the opportunity for novel therapeutic targets to dampen excitability in individuals who are susceptible to seizures.

In conclusion, these results provide strong evidence that NSW, such as that which occurs during the perimenstrual period, is associated with striking upregulation of the extrasynaptic δ-containing $GABA_A$Rs that mediate tonic inhibition in the hippocampus. This provides a molecular mechanism for enhanced anticonvulsant activity of neurosteroids and network inhibition in hyperexcitability conditions of catamenial epilepsy and other menstrual conditions linked to NSW. These findings provide a mechanistic rationale for neurosteroid therapy of catamenial epilepsy.

References

Agís-Balboa RC, Pinna G, Zhubi A, Maloku E, Veldic M, Costa E, Guidotti A (2006) Characterization of brain neurons that express enzymes mediating neurosteroid biosynthesis. Proc Natl Acad Sci U S A 103:14602–14607. CrossRef Medline

Belelli D, Lambert JJ (2005) Neurosteroids: endogenous regulators of the GABAA receptor. Nat Rev Neurosci 6:565–575. CrossRef Medline

Belelli D, Casula A, Ling A, Lambert JJ (2002) The influence of subunit composition on the interaction of neurosteroids with $GABA_A$ receptors. Neuropharmacology 43:651–661. CrossRef Medline

Bianchi MT, Macdonald RL (2003) Neurosteroids shift partial agonist activation of $GABA_A$ receptor channels from low- to high-efficacy gating patterns. J Neurosci 23:10934–10943. Medline

Brickley SG, Mody I (2012) Extrasynaptic GABA-A receptors: their function in the CNS and implications for disease. Neuron 73:23–34. CrossRef Medline

Bright DP, Renzi M, Bartram J, McGee TP, MacKenzie G, Hosie AM, Farrant M, Brickley SG (2011) Profound desensitization by ambient GABA limits activation of δ-containing $GABA_A$ receptors during spillover. J Neurosci 31:753–763. CrossRef Medline

Brown N, Kerby J, Bonnert TP, Whiting PJ, Wafford KA (2002) Pharmacological characterization of a novel cell line expressing human $\alpha4\beta3\delta$ GABAA receptors. Br J Pharmacol 136:965–974. CrossRef Medline

Carver CM, Reddy DS (2013) Neurosteroid interactions with synaptic and extrasynaptic $GABA_A$ receptors: regulation of subunit plasticity, phasic and tonic inhibition, and neuronal network excitability. Psychopharmacology 230:151–188. CrossRef Medline

Cherubini E, Conti F (2001) Generating diversity at GABAergic synapses. Trends Neurosci 24:155–162. CrossRef Medline

Cohen AS, Lin DD, Quirk GL, Coulter DA (2003) Dentate granule cell $GABA_A$ receptors in epileptic hippocampus: enhanced synaptic efficacy and altered pharmacology. Eur J Neurosci 17:1607–1616. CrossRef Medline

Coulter DA, Carlson GC (2007) Functional regulation of the dentate gyrus by GABA-mediated inhibition. Prog Brain Res 163:235–243. CrossRef Medline

DuBois DW, Damborsky JC, Fincher AS, Frye GD, Winzer-Serhan UH (2013) Varenicline and nicotine enhance GABAergic synaptic transmission in rat CA1 hippocampal and medial septum/diagonal band neurons. Life Sci 92:337–344. CrossRef Medline

Franklin KBJ, Paxinos G (1997) The mouse brain in stereotaxic coordinates, Ed 1. New York: Academic.

Gangisetty O, Reddy DS (2009) The optimization of TaqMan real-time RT-PCR assay for transcriptional profiling of $GABA_A$ receptor subunit plasticity. J Neurosci Methods 181:58–66. CrossRef Medline

Gangisetty O, Reddy DS (2010) Neurosteroid withdrawal regulates $GABA_A$ receptor α_4-subunit expression and seizure susceptibility by activation of progesterone receptor-independent early growth response factor-3 pathway. Neuroscience 170:865–880. CrossRef Medline

Glykys J, Mann EO, Mody I (2008) Which $GABA_A$ receptor subunits are necessary for tonic inhibition in the hippocampus? J Neurosci 28:1421–1426. CrossRef Medline

Harrison NL, Simmonds MA (1984) Modulation of the GABA receptor complex by a steroid anesthetic. Brain Res 323:287–292. CrossRef Medline

Herzog AG, Frye CA (2003) Seizure exacerbation associated with inhibition of progesterone metabolism. Ann Neurol 53:390–391. CrossRef Medline

Herzog AG, Harden CL, Liporace J, Pennell P, Schomer DL, Sperling M, Fowler K, Nikolov B, Shuman S, Newman M (2004) Frequency of catamenial seizure exacerbation in women with localization-related epilepsy. Ann Neurol 56:431–434. CrossRef Medline

Herzog AG, Fowler KM, Sperling MR, Liporace JD, Kalayjian LA, Heck CN, Krauss GL, Dworetzky BA, Pennel PB, Progesterone Trial Study Group (2011) Variation of seizure frequency with ovulatory status of menstrual cycles. Epilepsia 52:1843–1848. CrossRef Medline

Hosie AM, Wilkins ME, Smart TG (2007) Neurosteroid binding sites on $GABA_A$ receptors. Pharmacol Ther 116:7–19. CrossRef Medline

Houston CM, McGee TP, Mackenzie G, Troyano-Cuturi K, Rodriguez PM, Kutsarova E, Diamanti E, Hosie AM, Franks NP, Brickley SG (2012) Are extrasynaptic $GABA_A$ receptors important targets for sedative/hypnotic drugs? J Neurosci 32:3887–3897. CrossRef Medline

Jacob TC, Moss SJ, Jurd R (2008) $GABA_A$ receptor trafficking and its role in the dynamic modulation of neuronal inhibition. Nat Rev Neurosci 9:331–343. CrossRef Medline

Kay AR, Wong RK (1986) Isolation of neurons suitable for patch-clamping from adult mammalian central nervous systems. J Neurosci Methods 16:227–238. CrossRef Medline

Lerma J, Herranz AS, Herreras O, Abraira V, Martín del Río R (1986) In vivo determination of extracellular concentration of amino acids in the rat hippocampus. A method based on brain dialysis and computerized analysis. Brain Res 384:145–155. CrossRef Medline

Lydon JP, DeMayo FJ, Funk CR, Mani SK, Hughes AR, Montgomery CA Jr, Shyamala G, Conneely OM, O'Malley BW (1995) Mice lacking progesterone receptor exhibit pleiotropic reproductive abnormalities. Genes Dev 9:2266–2278. CrossRef Medline

Maguire J, Mody I (2007) Neurosteroid synthesis-mediated regulation of $GABA_A$ receptors: relevance to the ovarian cycle and stress. J Neurosci 27:2155–2162. CrossRef Medline

Maguire J, Mody I (2008) $GABA_A$R plasticity during pregnancy: relevance to postpartum depression. Neuron 59:207–213. CrossRef Medline

Maguire JL, Stell BM, Rafizadeh M, Mody I (2005) Ovarian cycle-linked changes in $GABA_A$ receptors mediating tonic inhibition alter seizure susceptibility and anxiety. Nat Neurosci 8:797–804. CrossRef Medline

Majewska MD, Harrison NL, Schwartz RD, Barker JL, Paul SM (1986) Steroid hormone metabolites are barbiturate-like modulators of the GABA receptor. Science 232:1004–1007. CrossRef Medline

Mangan PS, Sun C, Carpenter M, Goodkin HP, Sieghart W, Kapur J (2005) Cultured hippocampal pyramidal neurons express two kinds of $GABA_A$ receptors. Mol Pharmacol 67:775–788. CrossRef Medline

Meera P, Wallner M, Otis TS (2011) Molecular basis for the high THIP/gaboxadol sensitivity of extrasynaptic $GABA_A$ receptors. J Neurophysiol 106:2057–2064. CrossRef Medline

Mellon SH, Griffin LD, Compagnone NA (2001) Biosynthesis and action of neurosteroids. Brain Res Rev 37:3–12. CrossRef Medline

Mihalek RM, Banerjee PK, Korpi ER, Quinlan JJ, Firestone LL, Mi ZP, Lagenaur C, Tretter V, Sieghart W, Anagnostaras SG, Sage JR, Fanselow MS, Guidotti A, Spigelman I, Li Z, DeLorey TM, Olsen RW, Homanics GE (1999) Attenuated sensitivity to neuroactive steroids in γ-aminobutyrate type A receptor delta subunit knockout mice. Proc Natl Acad Sci U S A 96:12905–12910. CrossRef Medline

Minamoto Y, Itano T, Tokuda M, Matsui H, Janjua NA, Hosokawa K, Okada Y, Murakami TH, Negi T, Hatase O (1992) In vivo microdialysis of amino acid neurotransmitters in the hippocampus in amygdaloid kindled rat. Brain Res 573:345–348. CrossRef Medline

Moran MH, Smith SS (1998) Progesterone withdrawal I: pro-convulsant effects. Brain Res 807:84–90. CrossRef Medline

Moran MH, Goldberg M, Smith SS (1998) Progesterone withdrawal II: insensitivity to the sedative effects of a benzodiazepine. Brain Res 807:91–100.

Mortensen M, Ebert B, Wafford K, Smart TG (2010) Distinct activities of GABA agonists at synaptic- and extrasynaptic-type $GABA_A$ receptors. J Physiol 588:1251–1268. CrossRef Medline

Mtchedlishvili Z, Kapur J (2006) High-affinity, slowly desensitizing $GABA_A$ receptors mediate tonic inhibition in hippocampal dentate granule cells. Mol Pharmacol 69:564–575. CrossRef Medline

Mtchedlishvili Z, Sun CS, Harrison MB, Kapur J (2003) Increased neuroste-

roid sensitivity of hippocampal $GABA_A$ receptors during postnatal development. Neuroscience 118:655–666. CrossRef Medline

Nusser Z, Cull-Candy S, Farrant M (1997) Differences in synaptic $GABA_A$ receptor number underlie variation in GABA mini amplitude. Neuron 19:697–709. CrossRef Medline

Pack AM, Reddy DS, Duncan S, Herzog A (2011) Neuroendocrinological aspects of epilepsy: important issues and trends in future research. Epilepsy Behav 22:94–102. CrossRef Medline

Pandit S, Jeong JA, Jo JY, Cho HS, Kim DW, Kim JM, Ryu PD, Lee SY, Kim HW, Jeon BH, Park JB (2013) Dual mechanisms diminishing tonic $GABA_A$ inhibition of dentate gyrus granule cells in Noda epileptic rats. J Neurophysiol 110:95–102. CrossRef Medline

Pavlov I, Walker MC (2013) Tonic $GABA_A$ receptor-mediated signaling in temporal lobe epilepsy. Neuropharmacology 69:55–61. CrossRef Medline

Pavlov I, Huusko N, Drexel M, Kirchmair E, Sperk G, Pitkänen A, Walker MC (2011) Progressive loss of phasic, but not tonic GABA(A) receptor-mediated inhibition in dentate granule cells in a model of post-traumatic epilepsy in rats. Neuroscience 194:208–219. CrossRef Medline

Peng Z, Hauer B, Mihalek RM, Homanics GE, Sieghart W, Olsen RW, Houser CR (2002) $GABA_A$ receptor changes in δ subunit-deficient mice: altered expression of α4 and γ2 subunits in the forebrain. J Comp Neurol 446: 179–197. CrossRef Medline

Pillai GV, Smith AJ, Hunt PA, Simpson PB (2004) Multiple structural features of steroids mediate subtype-selective effects on human $\alpha4\beta3\delta$ $GABA_A$ receptors. Biochem Pharmacol 68:819–831. CrossRef Medline

Pirker S, Schwarzer C, Wieselthaler A, Sieghart W, Sperk G (2000) GABA(A) receptors: immunocytochemical distribution of 13 subunits in the adult rat brain. Neuroscience 101:815–850. CrossRef Medline

Racine RJ (1972) Modification of seizure activity by electrical stimulation. II. Motor seizure. Electroencephalogr Clin Neurophysiol 32:281–294. CrossRef Medline

Reddy DS (2009) The role of neurosteroids in the pathophysiology and treatment of catamenial epilepsy. Epilepsy Res 85:1–30. CrossRef Medline

Reddy DS (2011) Role of anticonvulsant and antiepileptogenic neurosteroids in the pathophysiology and treatment of epilepsy. Front Endocrinol (Lausanne) 2:38. CrossRef Medline

Reddy DS (2013) Neuroendocrine aspects of catamenial epilepsy. Horm Behav 63:254–266. CrossRef Medline

Reddy DS, Jian K (2010) The testosterone-derived neurosteroid androstanediol is a positive allosteric modulator of $GABA_A$ receptors. J Pharmacol Exp Ther 334:1031–1041. CrossRef Medline

Reddy DS, Mohan A (2011) Development and persistence of limbic epileptogenesis are impaired in mice lacking progesterone receptors. J Neurosci 31:650–658. CrossRef Medline

Reddy DS, Rogawski MA (2000) Enhanced anticonvulsant activity of ganaxolone after neurosteroid withdrawal in a rat model of catamenial epilepsy. J Pharmacol Exp Ther 294:909–915. Medline

Reddy DS, Rogawski MA (2001) Enhanced anticonvulsant activity of neuroactive steroids in a rat model of catamenial epilepsy. Epilepsia 42:337–344. CrossRef Medline

Reddy DS, Rogawski MA (2002) Stress-induced deoxycorticosterone-derived neurosteroids modulate GABA(A) receptor function and seizure susceptibility. J Neurosci 22:3795–3805. Medline

Reddy DS, Rogawski MA (2009) Neurosteroid replacement therapy for catamenial epilepsy. Neurotherapeutics 6:392–401. CrossRef Medline

Reddy DS, Zeng YC (2007) Effect of neurosteroid withdrawal on spontaneous recurrent seizures in a rat model of catamenial epilepsy. FASEB J 21:885.14. Medline

Reddy DS, Kim HY, Rogawski MA (2001) Neurosteroid withdrawal model of perimenstrual catamenial epilepsy. Epilepsia 42:328–336. CrossRef Medline

Reddy DS, Castaneda DC, O'Malley BW, Rogawski MA (2004) Anticonvulsant activity of progesterone and neurosteroids in progesterone receptor knockout mice. J Pharmacol Exp Ther 310:230–239. CrossRef Medline

Reddy DS, Gangisetty O, Briyal S (2010) Disease-modifying activity of progesterone in the hippocampus kindling model of epileptogenesis. Neuropharmacology 59:573–581. CrossRef Medline

Reddy DS, Gould J, Gangisetty O (2012) A mouse kindling model of perimenstrual catamenial epilepsy. J Pharmacol Exp Ther 341:784–793. CrossRef Medline

Reddy D, Ramanathan G (2012) Finasteride inhibits the disease-modifying activity of progesterone in the hippocampus kindling model of epileptogenesis. Epilepsy Behav 25:92–97. CrossRef Medline

Sanna E, Mostallino MC, Murru L, Carta M, Talani G, Zucca S, Mura ML, Maciocco E, Biggio G (2009) Changes in expression and function of extrasynaptic $GABA_A$ receptors in rat hippocampus during pregnancy and after delivery. J Neurosci 29:1755–1765. CrossRef Medline

Semyanov A, Walker MC, Kullmann DM, Silver RA (2004) Tonically active $GABA_A$ receptors: modulating gain and maintaining the tone. Trends Neurosci 27:262–269. CrossRef Medline

Shen H, Gong QH, Yuan M, Smith SS (2005) Short-term steroid treatment increases δ $GABA_A$ receptor subunit expression in rat CA1 hippocampus: pharmacological and behavioral effects. Neuropharmacology 49:573–586. CrossRef Medline

Shen H, Gong QH, Aoki C, Yuan M, Ruderman Y, Dattilo M, Williams K, Smith SS (2007) Reversal of neurosteroid effects at $\alpha4\beta2\delta$ $GABA_A$ receptors triggers anxiety at puberty. Nat Neurosci 10:469–477. CrossRef Medline

Smith SS, Gong QH (2005) Neurosteroid administration and withdrawal alter $GABA_A$ receptor kinetics in CA1 hippocampus of female rats. J Physiol 564:421–436. CrossRef Medline

Smith SS, Gong QH, Hsu FC, Markowitz RS, ffrench-Mullen JM, Li X (1998a) $GABA_A$ receptor α4 subunit suppression prevents withdrawal properties of an endogenous steroid. Nature 392:926–930. CrossRef Medline

Smith SS, Gong QH, Li X, Moran MH, Bitran D, Frye CA, Hsu FC (1998b) Withdrawal from 3α-OH-5α-pregnan-20-one using a pseudopregnancy model alters the kinetics of hippocampal $GABA_A$-gated current and increases the $GABA_A$ receptor α4 subunit in association with increased anxiety. J Neurosci 18:5275–5284. Medline

Smith SS, Shen H, Gong QH, Zhou X (2007) Neurosteroid regulation of $GABA_A$ receptors: focus on the α_4 and δ subunits. Pharmacol Ther 116: 58–76. CrossRef Medline

Spigelman I, Li Z, Liang J, Cagetti E, Samzadeh S, Mihalek RM, Homanics GE, Olsen RW (2003) Reduced inhibition and sensitivity to neurosteroids in hippocampus of mice lacking the $GABA_A$ receptor δ subunit. J Neurophysiol 90:903–910. CrossRef Medline

Stell BM, Brickley SG, Tang CY, Farrant M, Mody I (2003) Neuroactive steroids reduce neuronal excitability by selectively enhancing tonic inhibition mediated by δ subunit-containing GABAA receptors. Proc Natl Acad Sci U S A 100:14439–14444. CrossRef Medline

Stórustovu SI, Ebert B (2006) Pharmacological characterization of agonists at δ-containing $GABA_A$ receptors: functional selectivity for extrasynaptic receptors is dependent on the absence of γ_2. J Pharmacol Exp Ther 316: 1351–1359. CrossRef Medline

Sun C, Sieghart W, Kapur J (2004) Distribution of α_1, γ_2, and δ subunits of $GABA_A$ receptors in hippocampal granule cells. Brain Res 1029:207–216. CrossRef Medline

Sun C, Mtchedlishvili Z, Erisir A, Kapur J (2007) Diminished neurosteroid sensitivity of synaptic inhibition and altered location of the α_4 subunit of GABA-$_A$ receptors in an animal model of epilepsy. J Neurosci 27:12641–12650. CrossRef Medline

Sundstrom-Poromaa I, Smith DH, Gong QH, Sabado TN, Li X, Light A, Wiedmann M, Williams K, Smith SS (2002) Hormonally regulated $\alpha_4\beta_2\delta$ $GABA_A$ receptors are a target for alcohol. Nat Neurosci 5:721–722. CrossRef Medline

Tuveri A, Paoletti AM, Orrù M, Melis GB, Marotto MF, Zedda P, Marrosu F, Sogliano C, Marra C, Biggio G, Concas A (2008) Reduced serum level of THDOC, an anticonvulsant steroid, in women with perimenstrual catamenial epilepsy. Epilepsia 49:1221–1229. CrossRef Medline

Wei W, Zhang N, Peng Z, Houser CR, Mody I (2003) Perisynaptic localization of δ subunit-containing $GABA_A$ receptors and their activation by GABA spillover in the mouse dentate gyrus. J Neurosci 23:10650–10661. Medline

Wohlfarth KM, Bianchi MT, Macdonald RL (2002) Enhanced neurosteroid potentiation of ternary $GABA_A$ receptors containing the δ subunit. J Neurosci 22:1541–1549. Medline

Wu X, Gangisetty O, Carver CM, Reddy DS (2013) Estrous cycle regulation of extrasynaptic δ-containing $GABA_A$ receptor-mediated tonic inhibition and limbic epileptogenesis. J Pharmacol Exp Ther 346:146–160. CrossRef Medline

Zhang N, Wei W, Mody I, Houser CR (2007) Altered localization of $GABA_A$ receptor subunits on dentate granule cell dendrites influences tonic and phasic inhibition in a mouse model of epilepsy. J Neurosci 27:7520–7531. CrossRef Medline